中国科学院上海应用物理研究所
Shanghai Institute of Applied Physics, Chinese Academy of Sciences

Strangeness production in RHIC beam energy scan

Yu-Gang Ma

Shanghai Institute of Applied Physics, CAS

"Strangeness Nuclear Physics 2017, Osaka, Japan; March 12-14, 2017

Outline

- Strangeness production in heavy ion collisions
- Strangeness measurements in STAR
  - ✓ Beam energy scan: Au+Au 7.7 – 200 GeV
  - ✓ Flow of multi-strange particle
  - ✓ Lambda polarization
- Lifetime measurement of hypertriton
- Summary

Strangeness

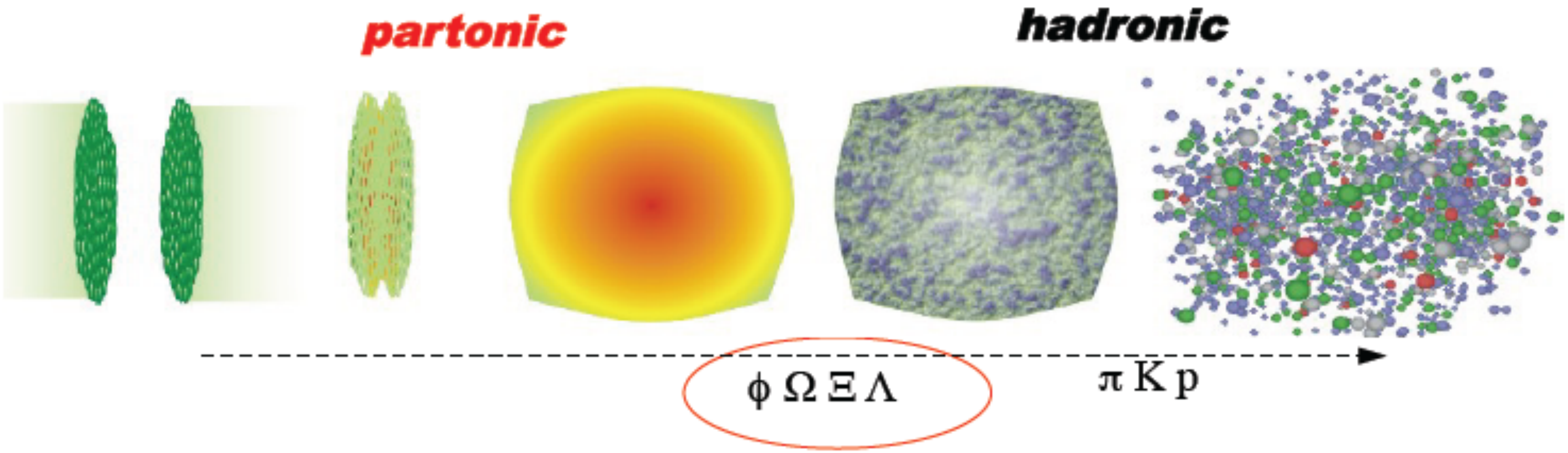

- **Strange, multi-strange hadrons and ϕ meson**
  Less sensitive to late hadronic interactions
- **Ω hyperons and ϕ meson**
  minimal distortion from decay feed-down

Good probe for QGP properties and QCD phase transition

- ***Key observables***
- **Event anisotropy v_2**
  Collectivity
- **Nuclear modification factor**
  Partonic energy loss and recombination
- **Baryon/meson ratio**
  Parton recombination

STAR measurements at the beam energies of 7.7, 11.5, 14.5, 19.6, 27, 39, 62.4 and 200 GeV

Strangeness in Quark-Gluon Plasma

"Strangeness Production in the Quark-Gluon Plasma", by J. Rafelski and B. Muller, PRL 48 (1982) 1066, cited > 600
"Strangeness in relativistic heavy ion collisions", by P. Koch, B. Muller and J. Rafelski, Phys. Rept. 142 (1986) 167, cited > 730

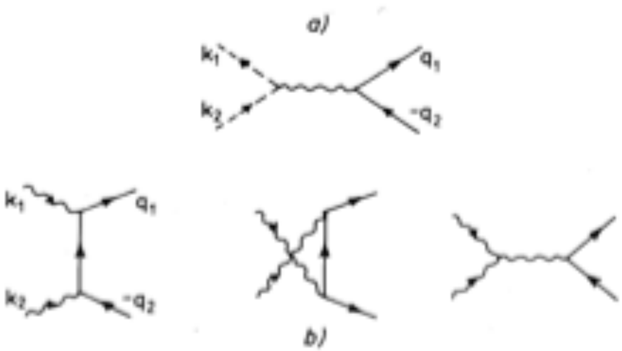

FIG. 1. Lowest-order QCD diagrams for $s\bar{s}$ production: (a) $q\bar{q}\to s\bar{s}$, (b) $gg\to s\bar{s}$.

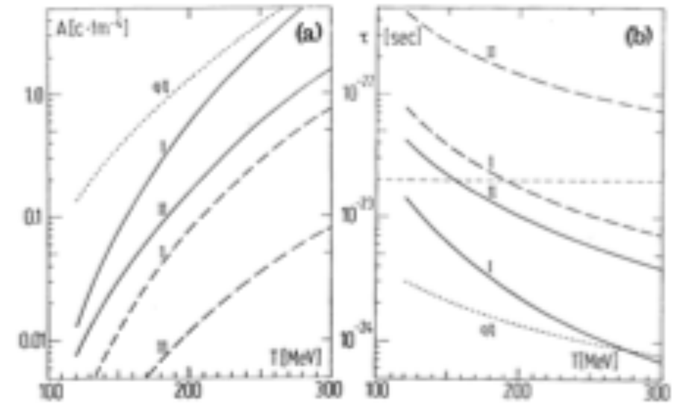

FIG. 2. (a) Rates A. (b) Time constants τ as functions of temperature T. Full lines, $q\bar{q}\to s\bar{s}$ and $gg\to s\bar{s}$; dashed lines, $q\bar{q}\to s\bar{s}$; dotted lines, $gg\to q\bar{q}$ ($M = 15$ MeV). Curves marked I are for $\alpha_s = 2.2$ and $M = 280$ MeV; those marked II are for $\alpha_s = 0.6$ and $M = 150$ MeV.

Strangeness Production: (J.Rafelski and B. Muller PRL 48, 1066 (1982))

s-$\bar{s}$ quark pair production from gluon fusions in QGP leads to strangeness equilibration in QGP → most prominent in strange hyperon production (Λ,Ξ,Ω and anti-particles).

$$dn_s/dt = A\{1-[n_s(t)/n_s(\infty)]^2\},$$

$$n_s(t) = n_s(\infty)\tanh(t/\tau), \quad \tau = n_s(\infty)/A.$$

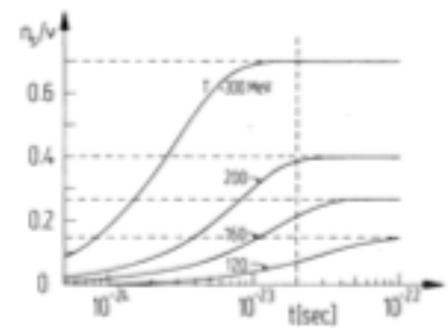

FIG. 3. Time evolution of the relative strange-quark to baryon-number abundance in the plasma for various temperatures ($M = 150$ MeV, $\alpha_s = 0.6$).

"Strangeness abundance saturates in sufficiently excited QGP (T> 160 MeV, E> 1 GeV/fm^3), allowing to utilise enhanced abundances of rare, strange hadrons as indicators for the formation of the plasma state in nuclear collisions."

s quarks: good probe for QCD phase transition & QGP properties

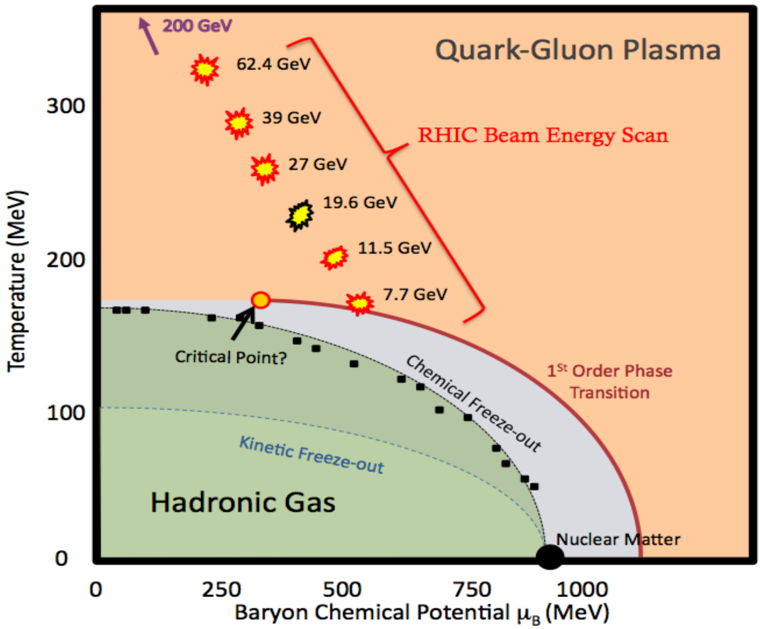

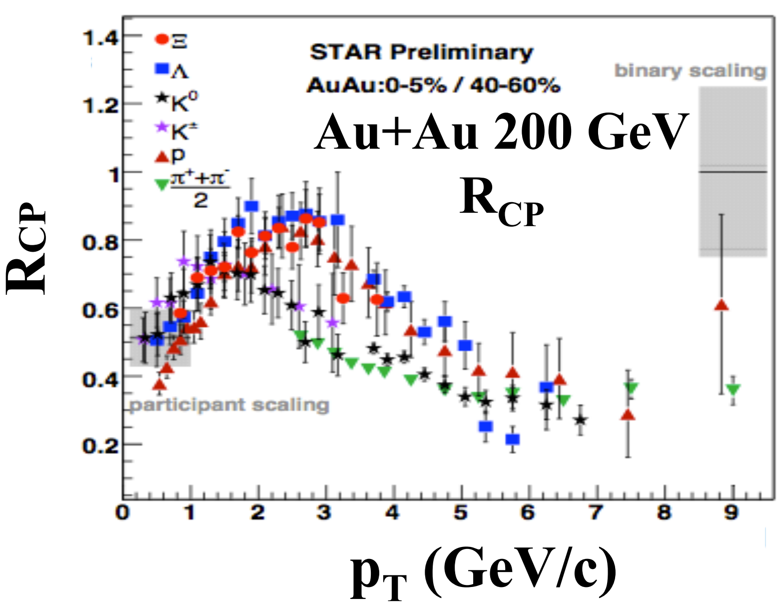

- **Beam Energy Scan at RHIC**
  Au+Au collisions *at 7.7, 11.5, 14.5, 19.6, 27, 39, 62.4, 200 GeV*
  Look for **onset of de-confinement, phase boundary** and critical point

- Key observables
  (1) Strangeness enhancement
  (2) Baryon/meson ratio
  Parton recombination
  (3) Nuclear modification factor
  Partonic energy loss & recombination

STAR, arXiv:1007.2613; NA49, PRC78, 034918

Relativistic Heavy Ion Collider (RHIC)

Focus on the STAR Detector

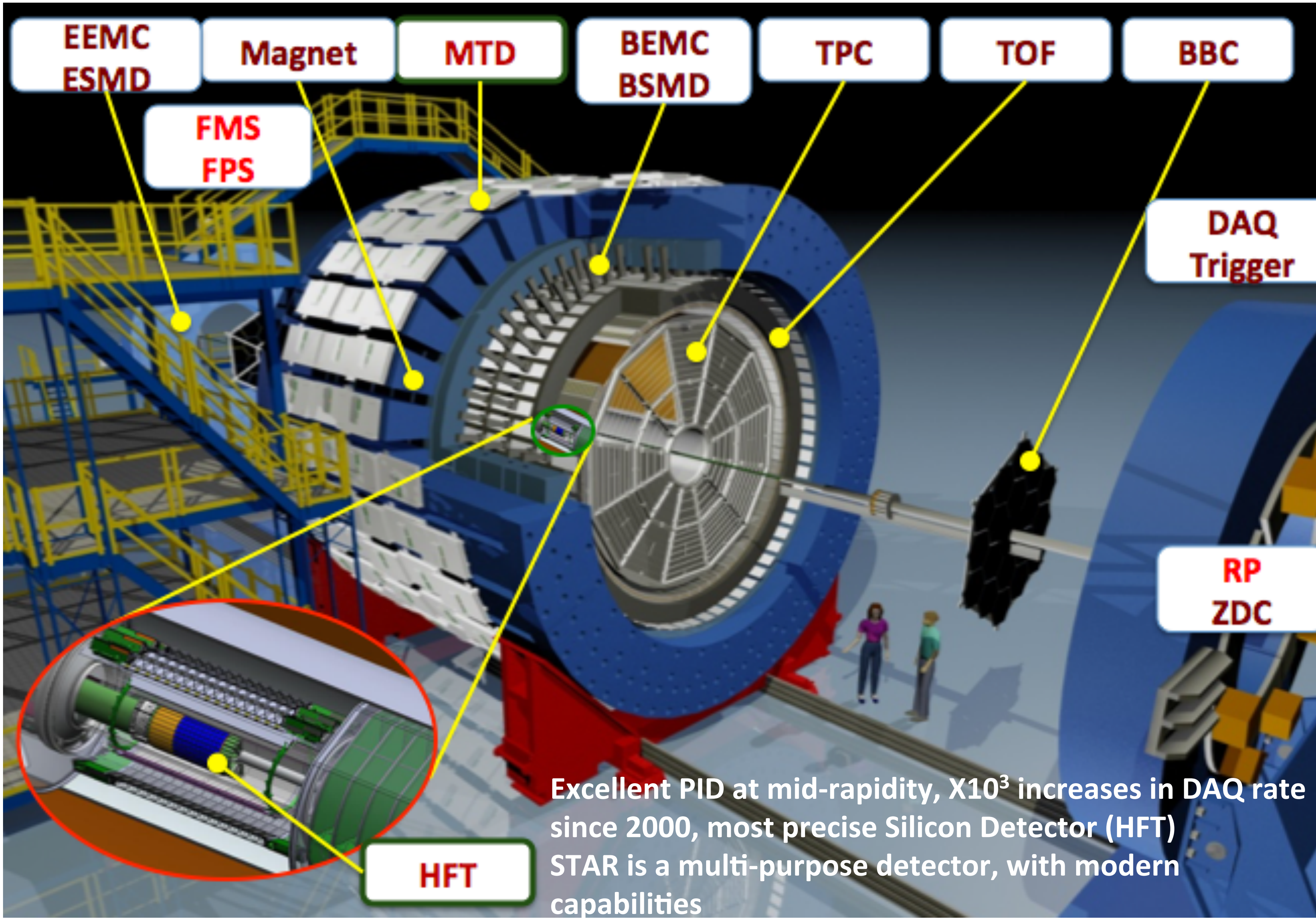

Excellent PID at mid-rapidity, X10^3 increases in DAQ rate since 2000, most precise Silicon Detector (HFT)
STAR is a multi-purpose detector, with modern capabilities

Detector settings and data sets

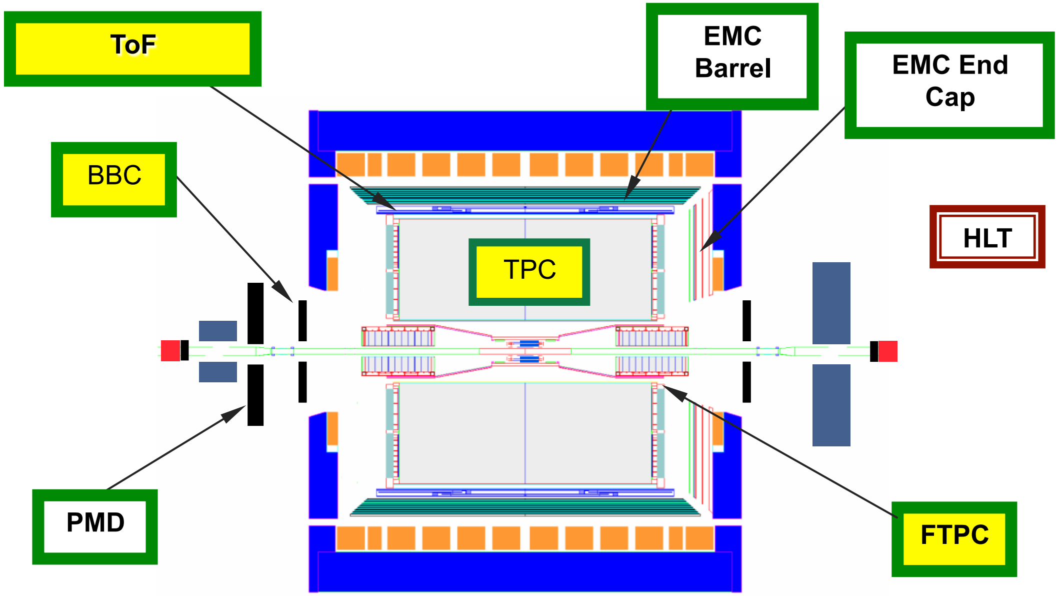

Year	*Collisions*	$\sqrt{s_{NN}}$ (GeV)	MB events in Million
2010	Au+Au	7.7	~ 4 M
2010	Au+Au	11.5	~ 12 M
2014	Au+Au	14.5	~ 18 M
2011	Au+Au	19.6	~ 36 M
2011	Au+Au	27	~ 70 M
2010	Au+Au	39	~ 130 M
2011	Au+Au	200	~ 480 M
2012	U+U	193	~ 270 M
2009	p+p	200	~ 107 M

Strangeness particles reconstructed in STAR

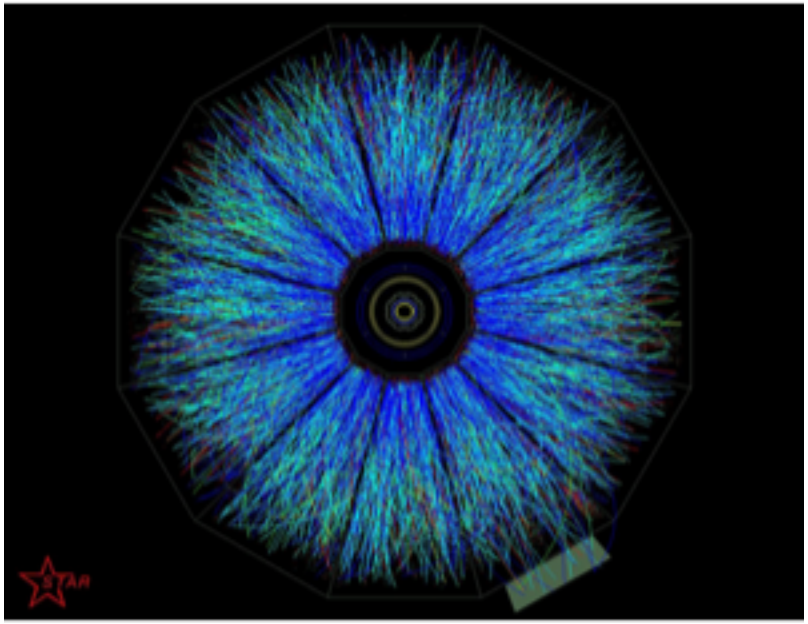

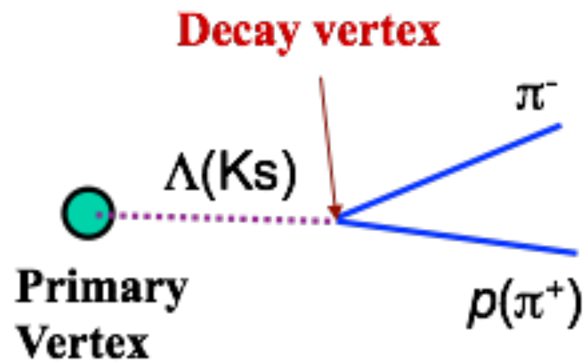

$K_S \rightarrow \pi^+\pi^-$ ($\Gamma_i/\Gamma \approx$ 69%), $c\tau$ = 2.69cm

$\Lambda \rightarrow p\pi^-$ ($\Gamma_i/\Gamma \approx$ 64%), $c\tau$ = 7.89cm

$\Xi^- \rightarrow \Lambda\pi^-$ ($\Gamma_i/\Gamma \approx$ 99.9%), $c\tau$ = 4.91cm

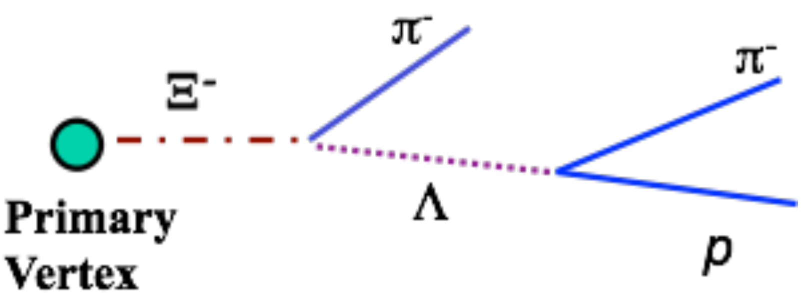

$$m = \sqrt{(\sqrt{m_+^2 + P_+^2} + \sqrt{m_-^2 + P_-^2})^2 - P^2},$$

Particle identification and reconstruction

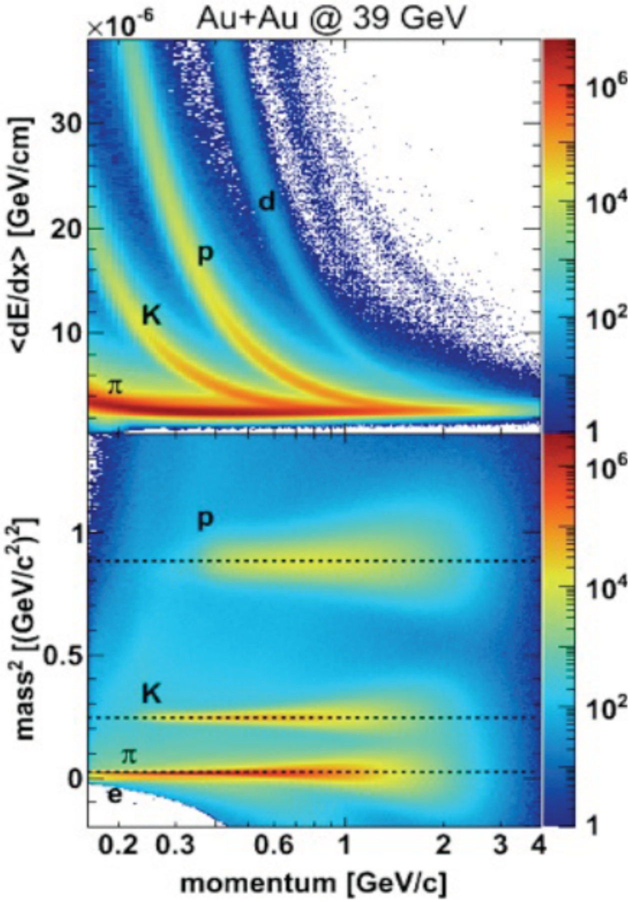

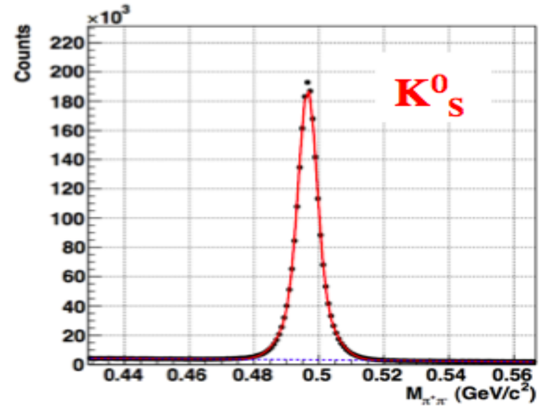

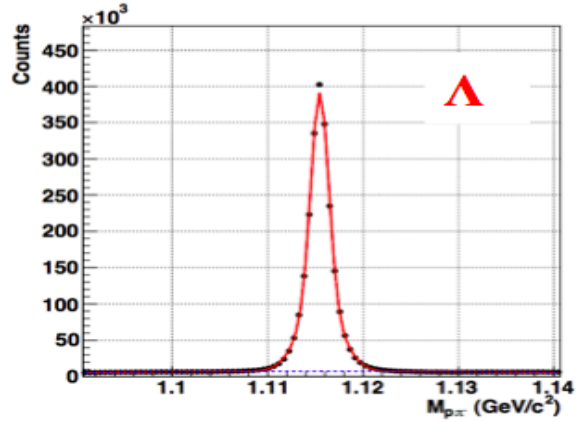

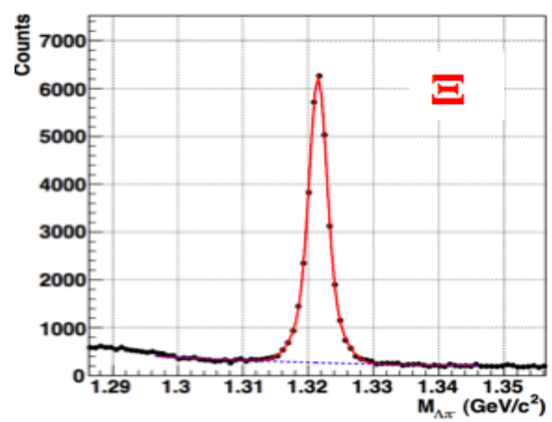

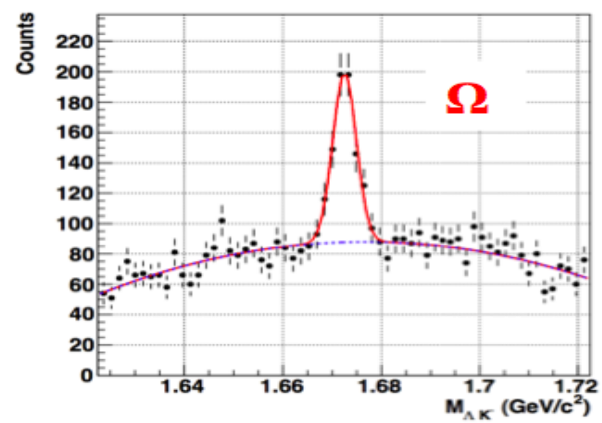

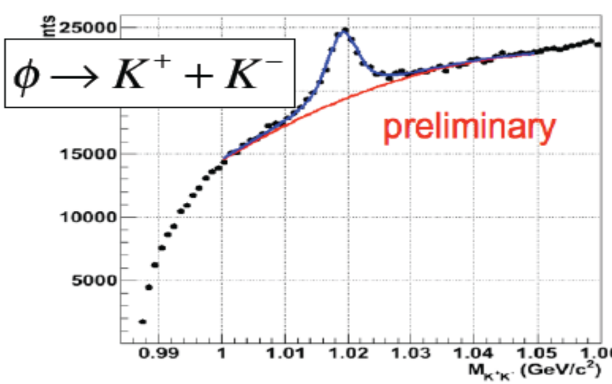

- dE/dx+TOF: π, K, p and $\phi \rightarrow K^+ + K^-$ (invariant mass)
- Weak decay particles (K^0_S, Λ, Ξ, Ω), secondary vertex + invariant mass

Invariant Yield

π^+

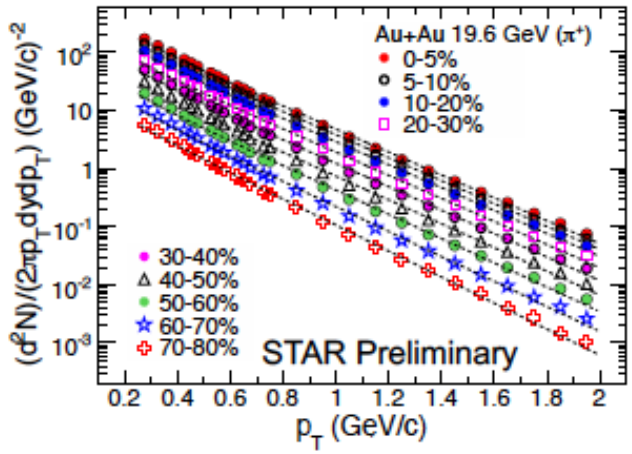

K^+

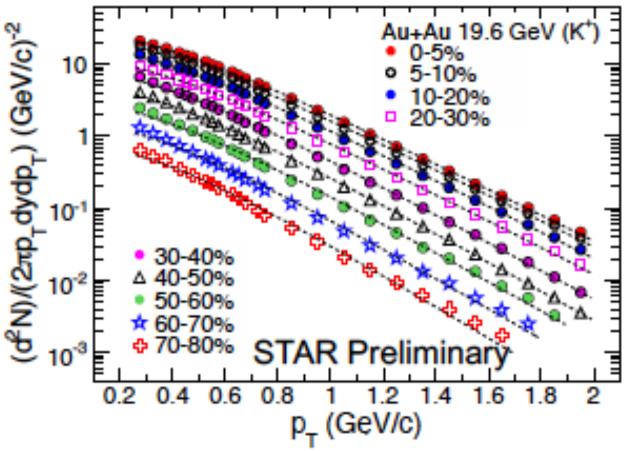

p

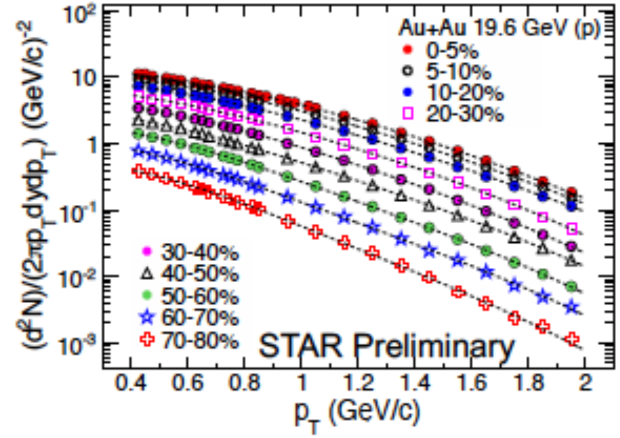

Pion curves:
Bose-Einstein fits

Au+Au 19.6 GeV

Kaon curves:
$(m_T\text{-}m)$ exponential fits

proton curves:
Double exponential fits

π^-

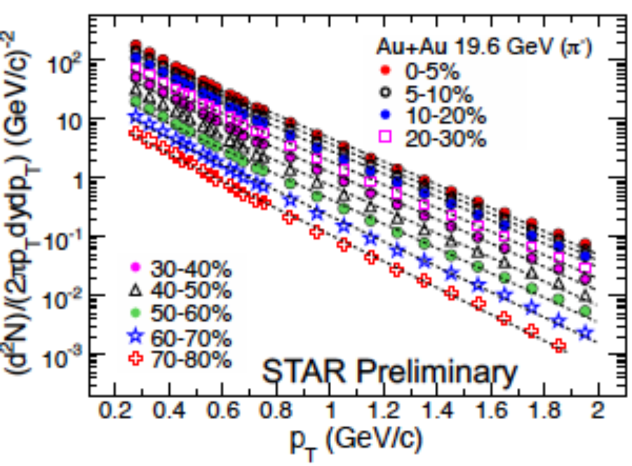

K^-

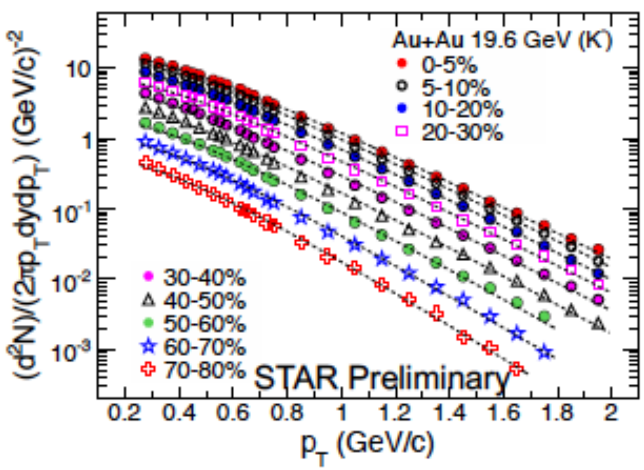

pbar

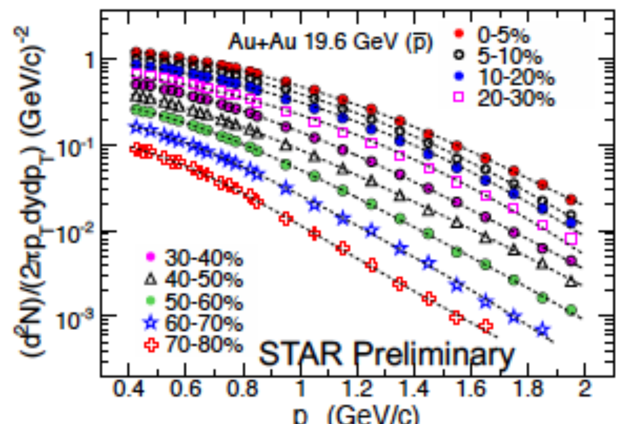

Spectra are characterized by dN/dy and $<p_T>$ or $<m_T>$

p_T spectra (K ^S↑0↓ , Λ, Ξ at 39 GeV)

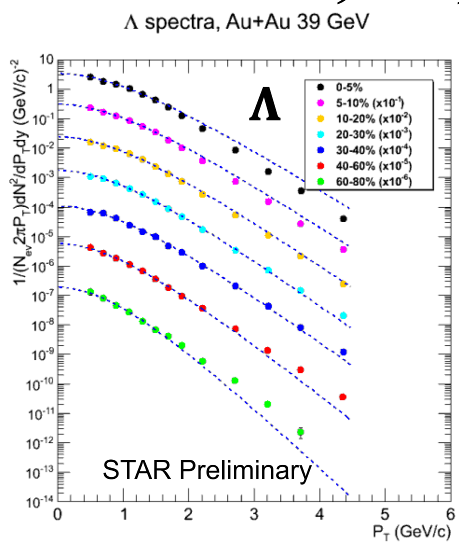

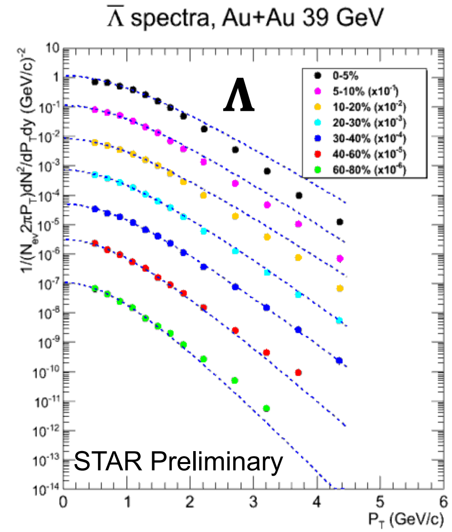

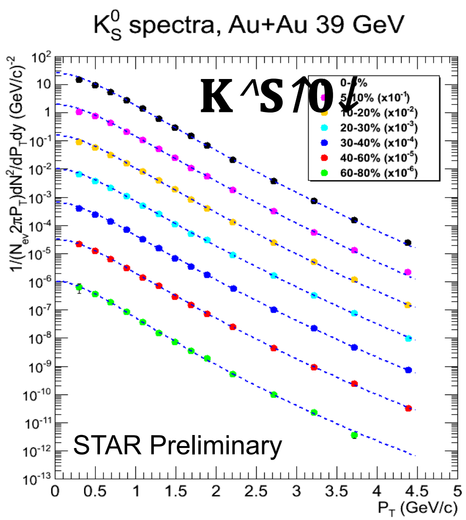

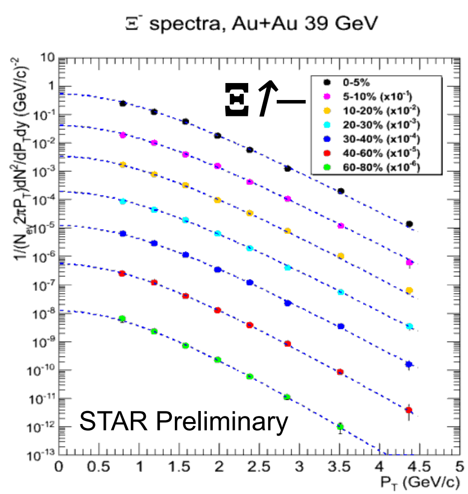

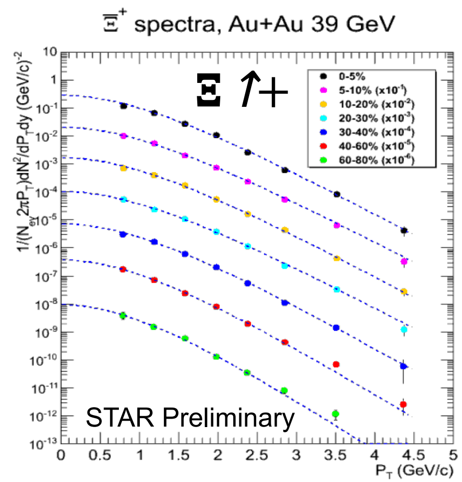

- Extensive strange particle spectra

Statistical error

- Λ(Λ) **spectra are weak decay feed-down corrected**

~ 20% for Λ; ~ 25% for Λ

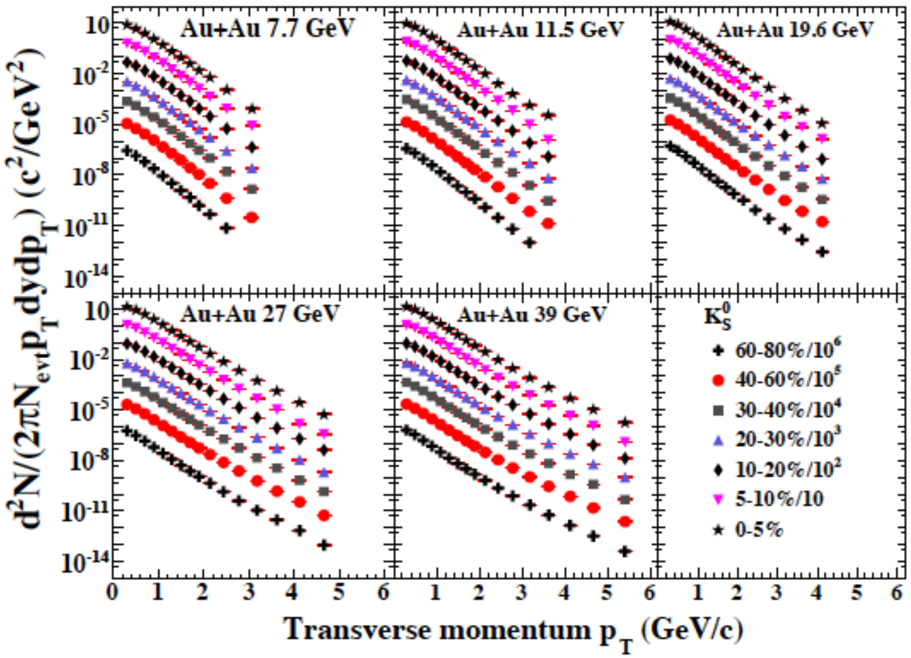
Au+Au 7.7 GeV
Au+Au 11.5 GeV
Au+Au 19.6 GeV
Au+Au 27 GeV
Au+Au 39 GeV
K^0_S
60-80%/10^6
40-60%/10^5
30-40%/10^4
20-30%/10^3
10-20%/10^2
5-10%/10
0-5%
$d^2N/(2\pi N_{evt} p_T dy dp_T)$ (c^2/GeV^2)
Transverse momentum p_T (GeV/c)

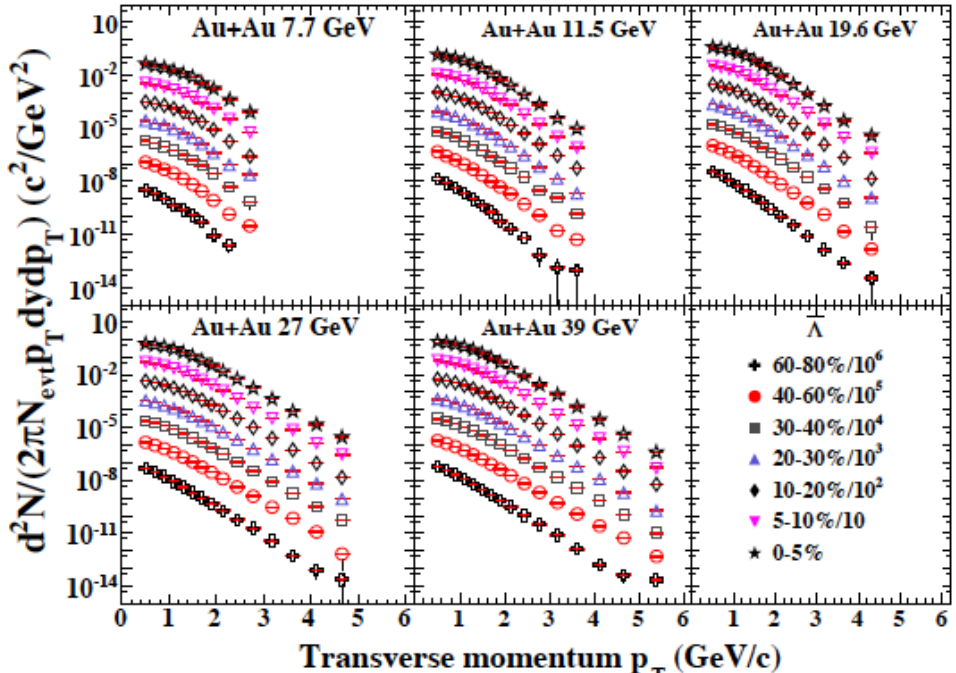
Au+Au 7.7 GeV
Au+Au 11.5 GeV
Au+Au 19.6 GeV
Au+Au 27 GeV
Au+Au 39 GeV
$\bar{\Lambda}$
60-80%/10^6
40-60%/10^5
30-40%/10^4
20-30%/10^3
10-20%/10^2
5-10%/10
0-5%
$d^2N/(2\pi N_{evt} p_T dy dp_T)$ (c^2/GeV^2)
Transverse momentum p_T (GeV/c)

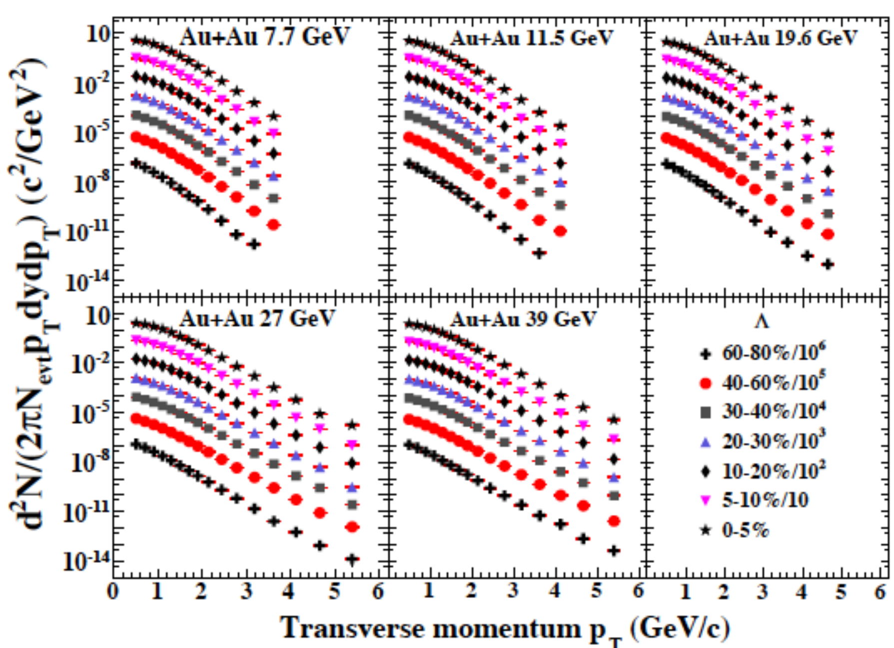
Au+Au 7.7 GeV
Au+Au 11.5 GeV
Au+Au 19.6 GeV
Au+Au 27 GeV
Au+Au 39 GeV
Λ
60-80%/10^6
40-60%/10^5
30-40%/10^4
20-30%/10^3
10-20%/10^2
5-10%/10
0-5%
$d^2N/(2\pi N_{evt} p_T dy dp_T)$ (c^2/GeV^2)
Transverse momentum p_T (GeV/c)

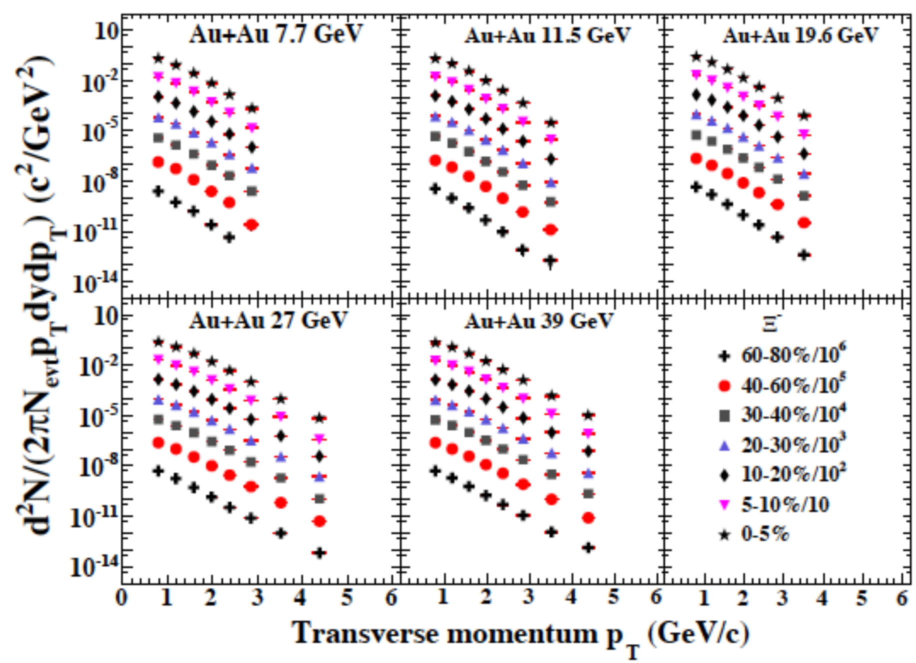
Au+Au 7.7 GeV
Au+Au 11.5 GeV
Au+Au 19.6 GeV
Au+Au 27 GeV
Au+Au 39 GeV
Ξ^-
60-80%/10^6
40-60%/10^5
30-40%/10^4
20-30%/10^3
10-20%/10^2
5-10%/10
0-5%
$d^2N/(2\pi N_{evt} p_T dy dp_T)$ (c^2/GeV^2)
Transverse momentum p_T (GeV/c)

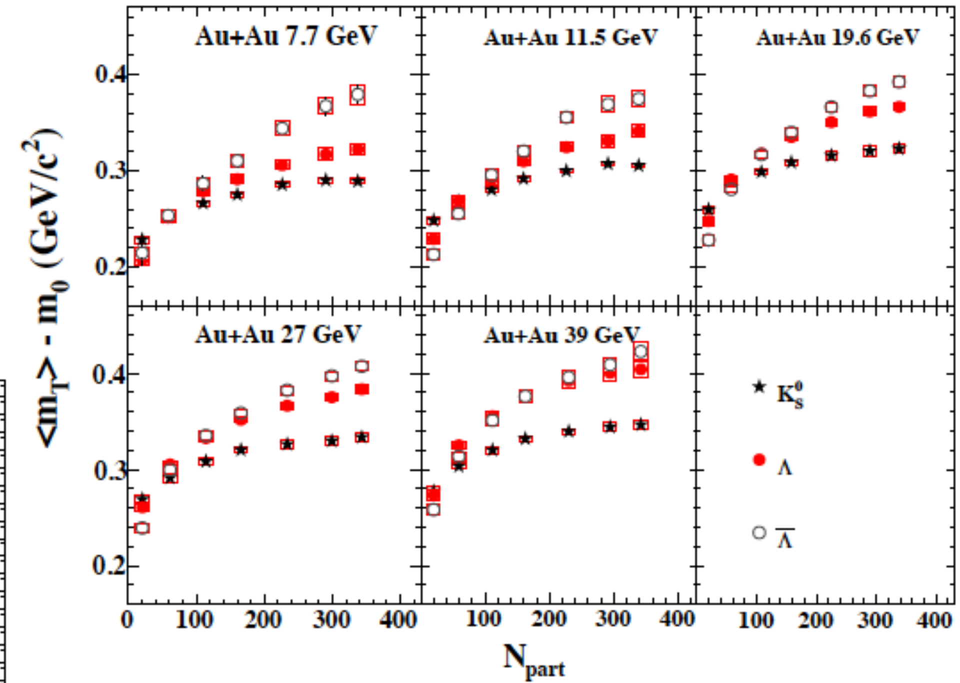

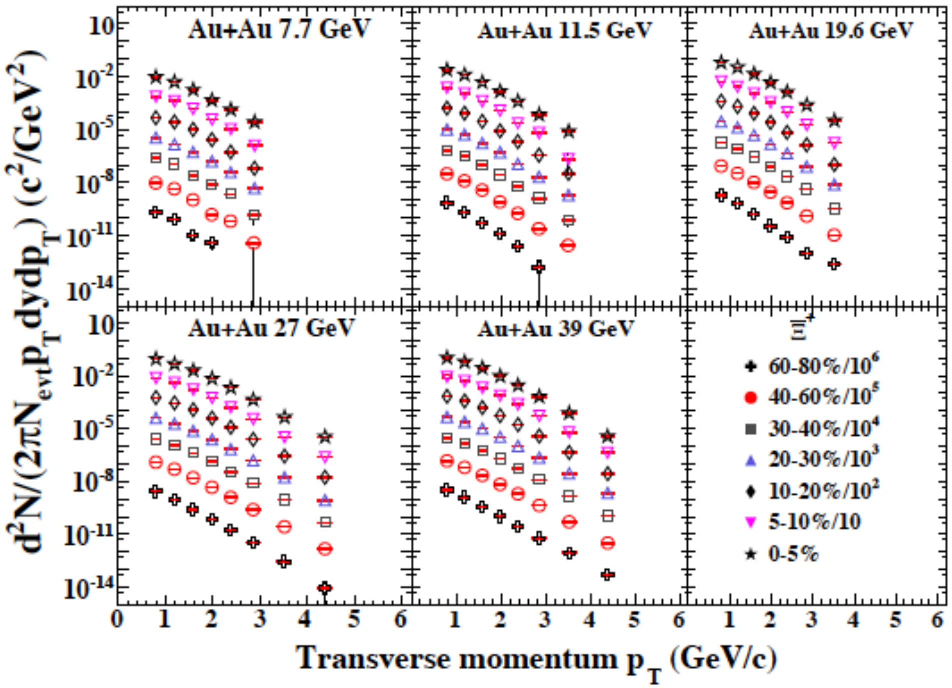

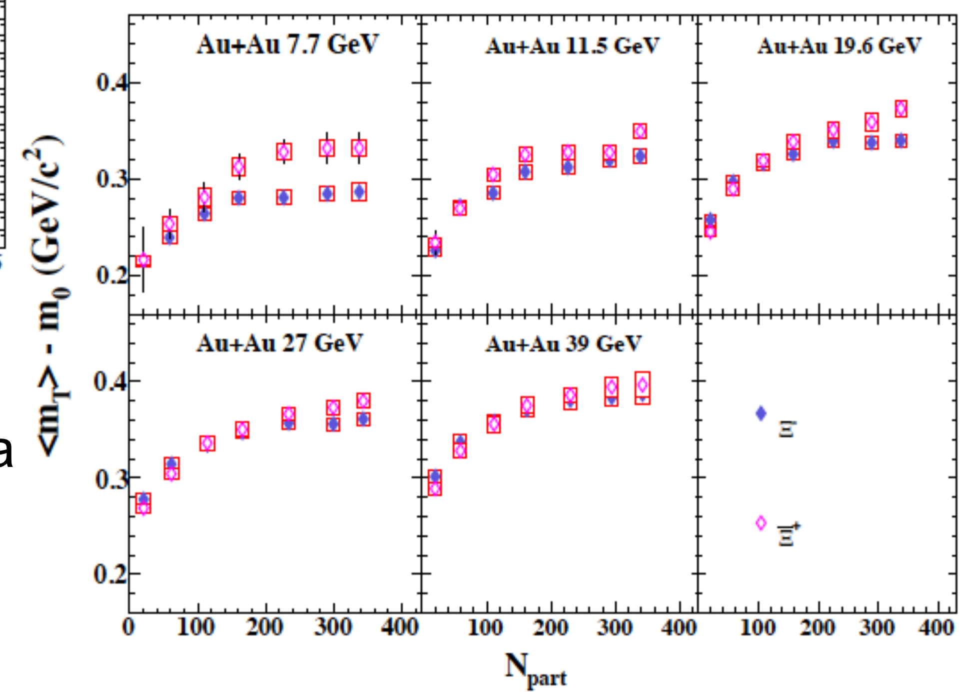

The striking feature of the <mT−m0> at beam energy scan is that there is a sizable difference between L and L-bar at lower energies.

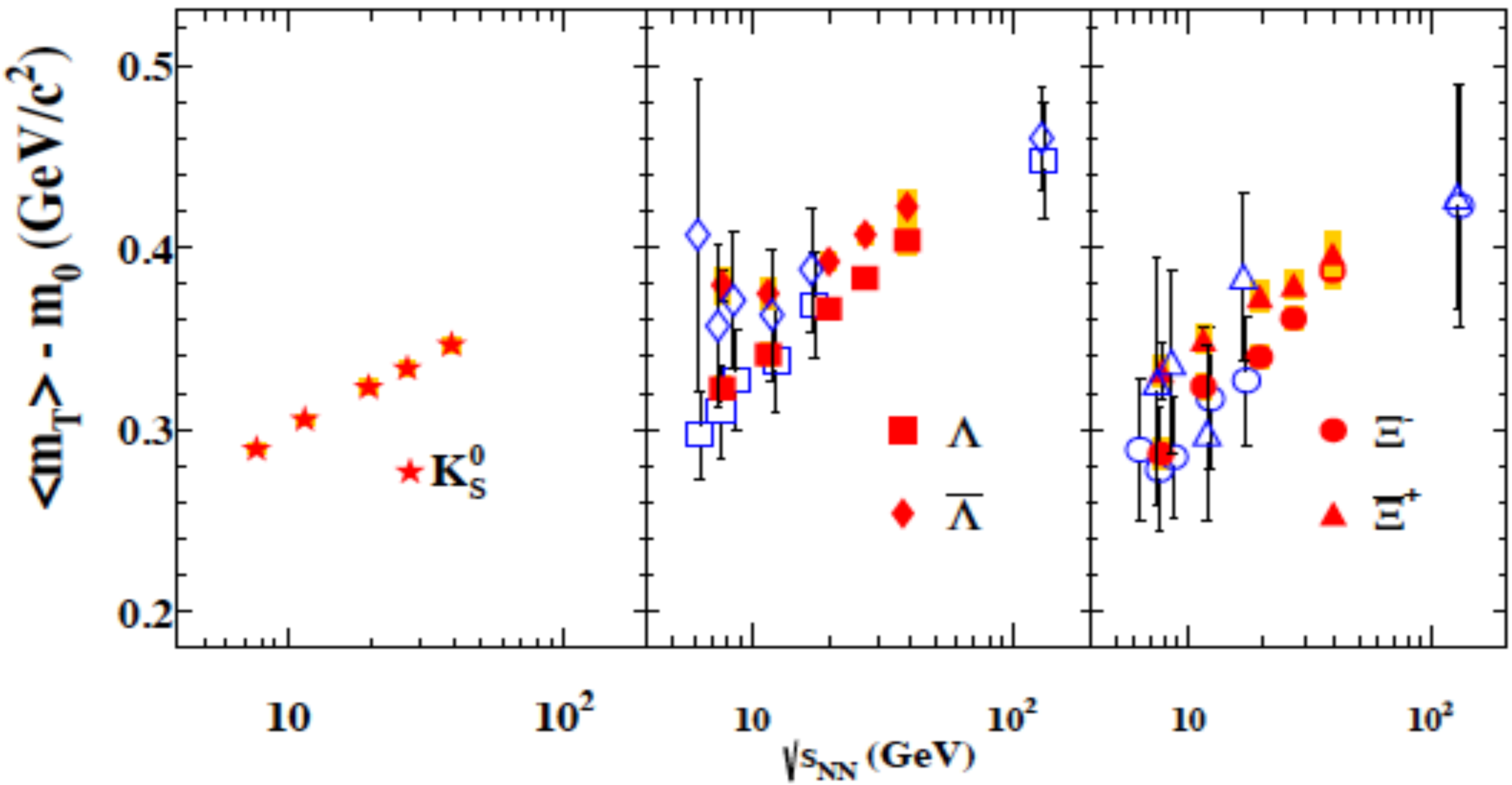

<mT−m0> vs beam energy: ia sizable difference between L and L-bar, Cas-Cas-bar at lower energies.

p_T spectra (Ω and ϕ)

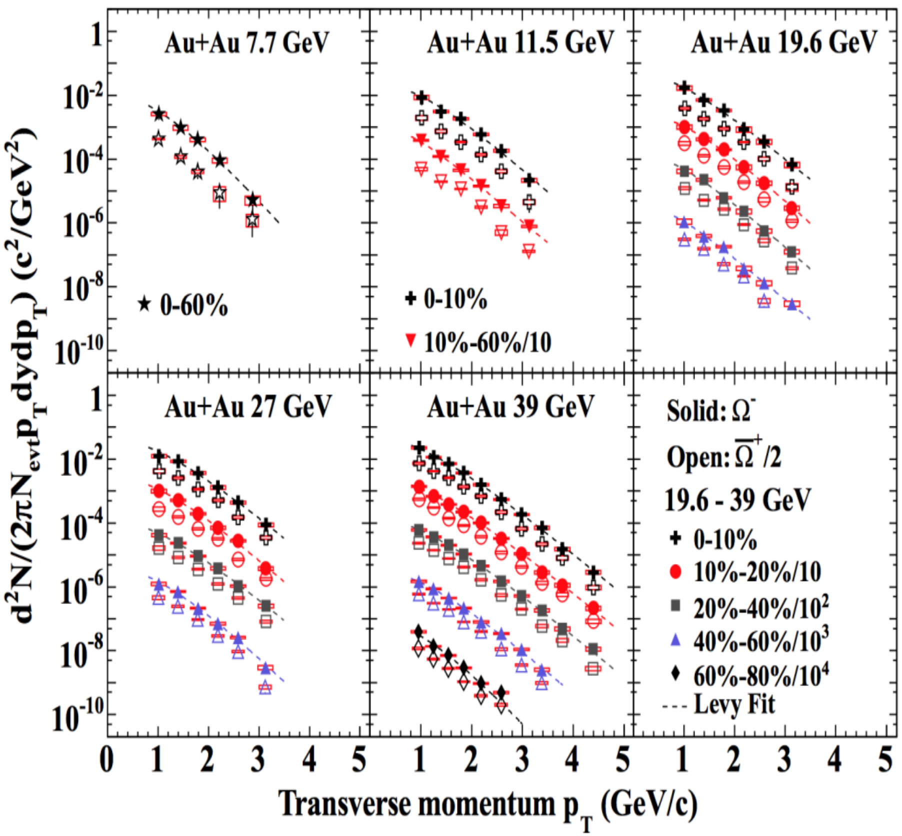

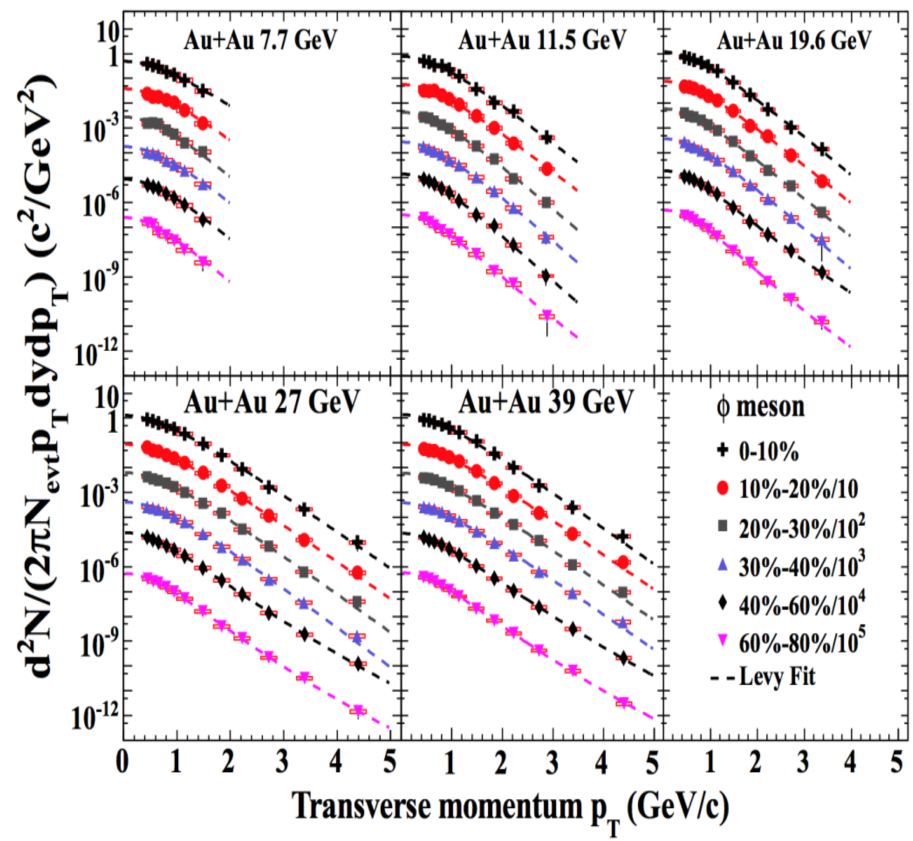

STAR, Phys. Rev. C 93, 2016, 021903 (R)

- Extensive strange particle spectra

Particle yields

mid-rapidity, most central collisions (0-5%)

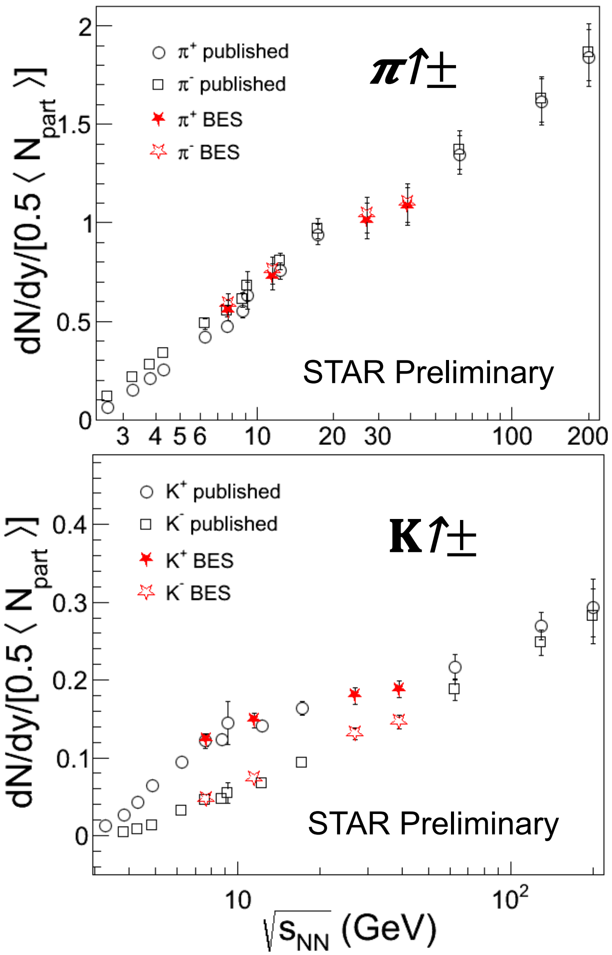

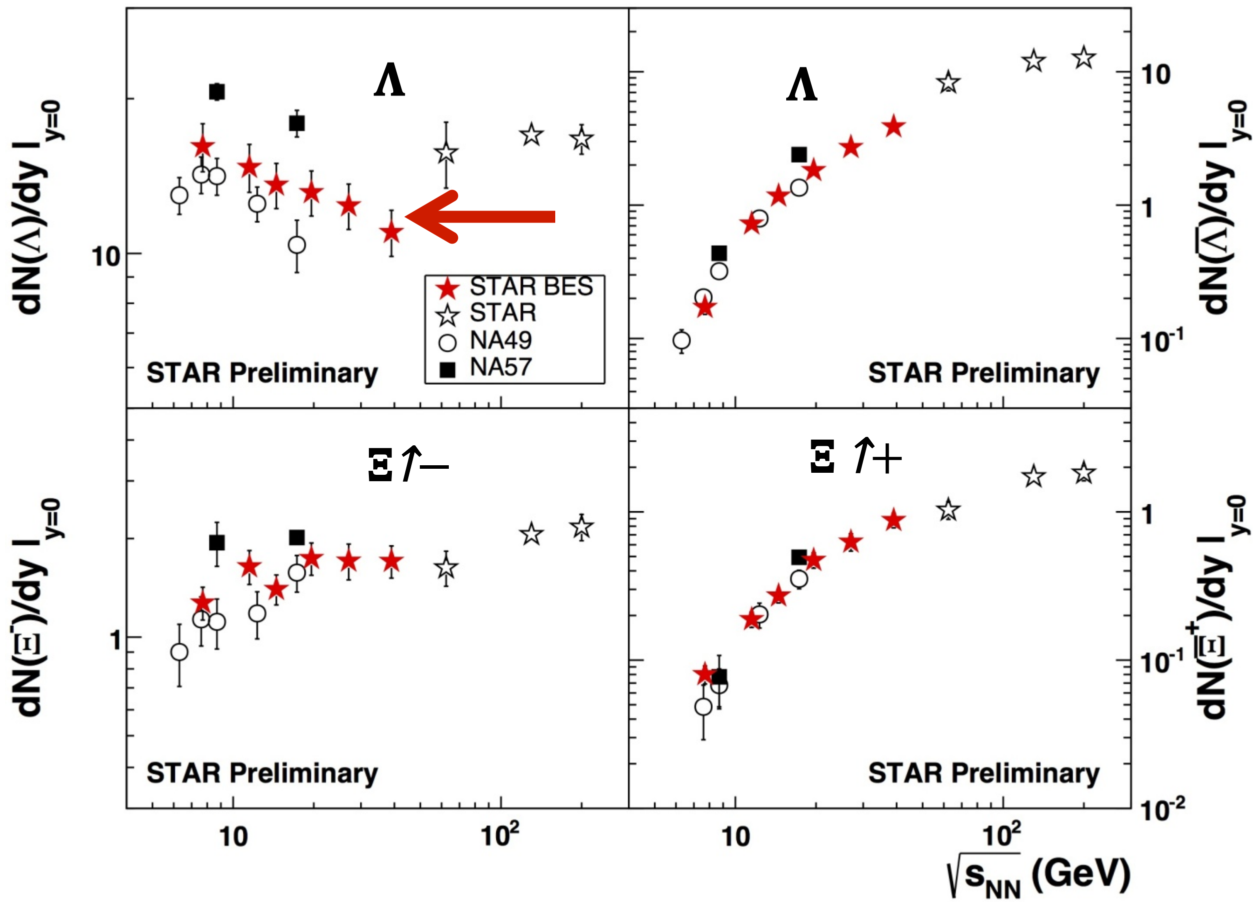

- STAR results are consistent with published data in general
- Λ yields seem to show dip around $\sqrt{s_{NN}}$ = 39 GeV. **The baryon stopping at mid-rapidity decreases with increasing energy**

Particle ratios

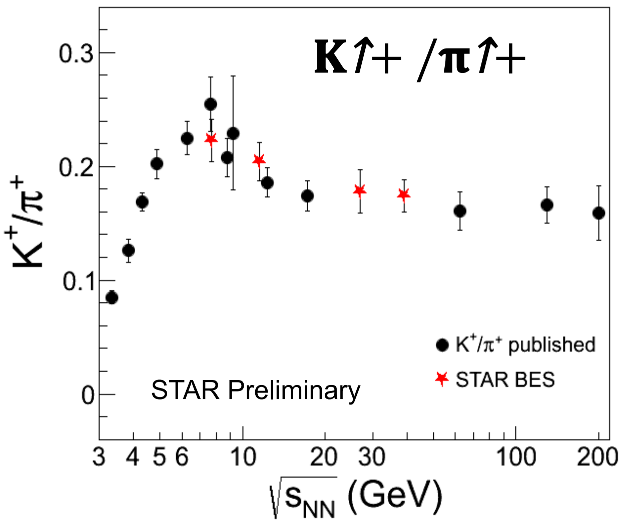

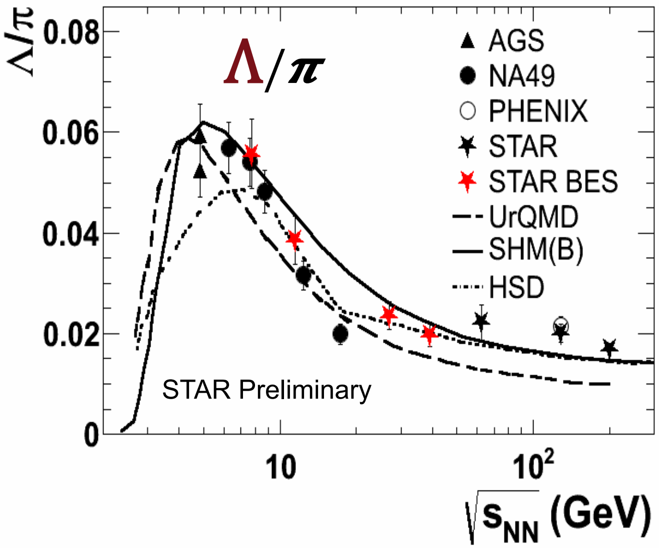

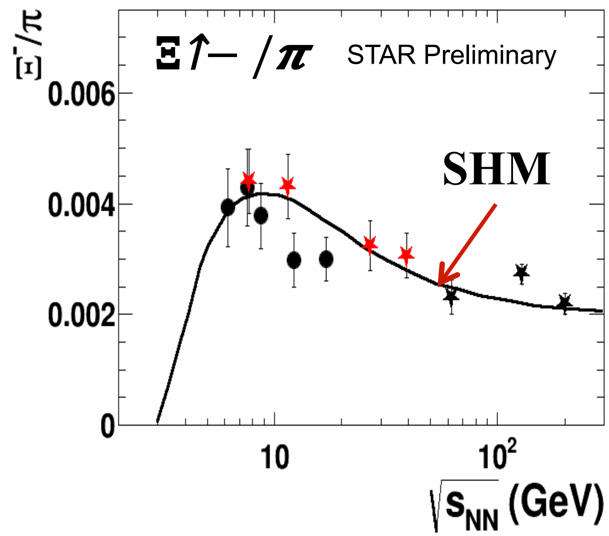

***most central (0-5%)**, mid-rapidity, stat. + sys. error*

RHIC BES

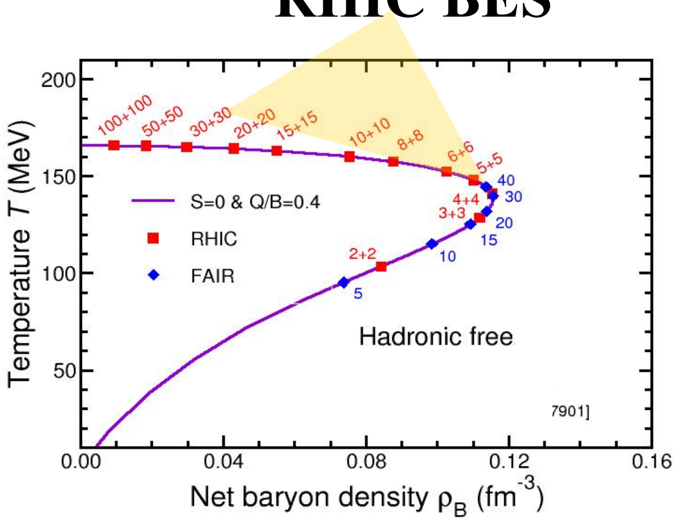

J. Randrup et al., PRC 74, 047901 (2006)

- Particle ratios consistent with NA49, consistent with the picture of a **maximum net-baryon density around $\sqrt{s_{NN}} \sim 8$ GeV at freeze-out**

Strangeness Enhancement

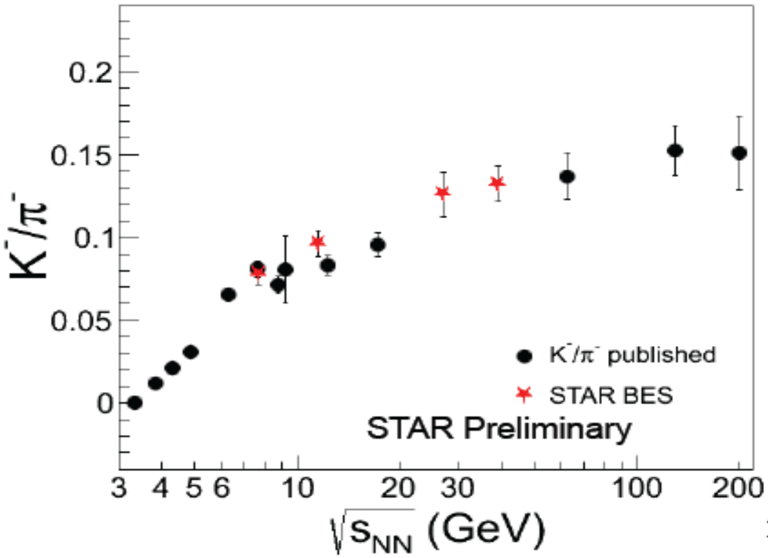

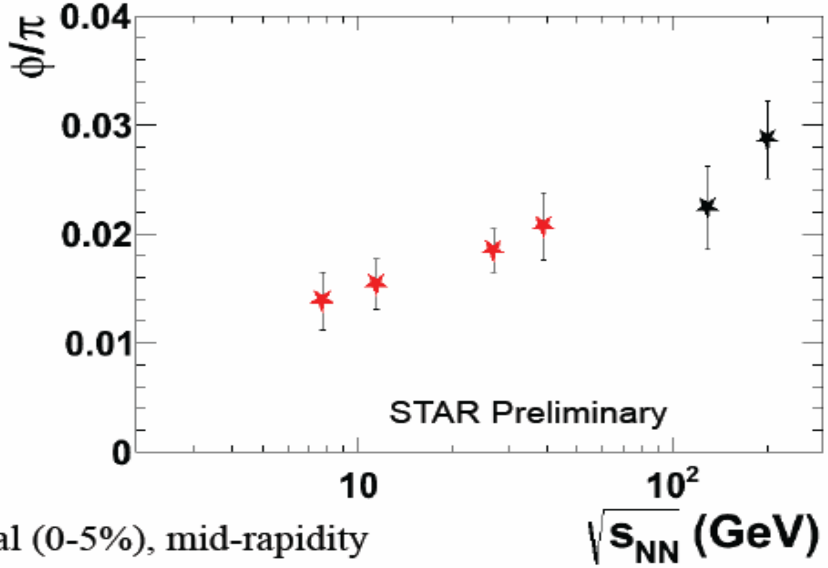

most central (0-5%), mid-rapidity

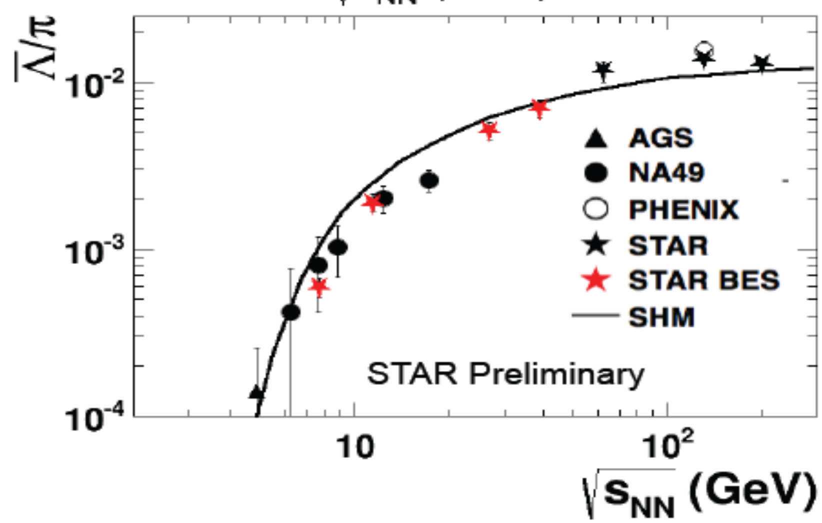

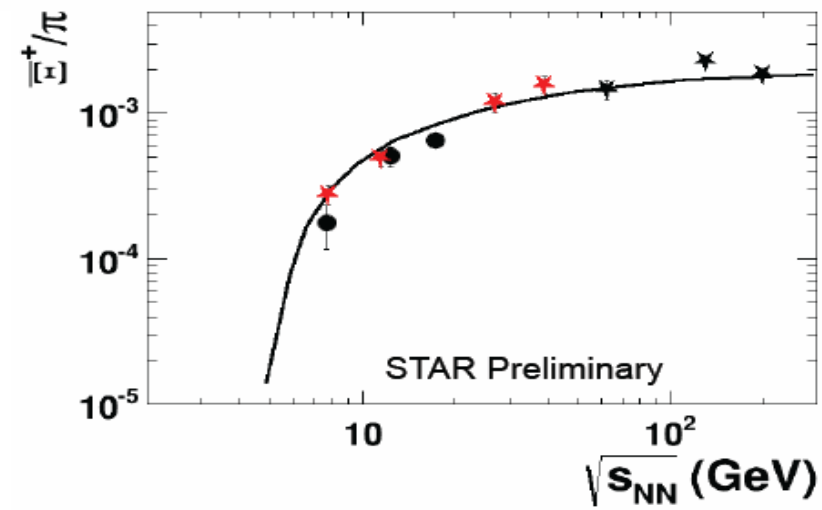

Statistical Hadron gas Model: A. Andronic et al., Nucl. Phys. A 772, 167 (2006)

- K^-, anti-Λ, anti-Ξ and ϕ yields increase significantly with respect to the pion yield as the beam energy increases

antibaryon/baryon ratios

Stopping, Thermalization and Absorption

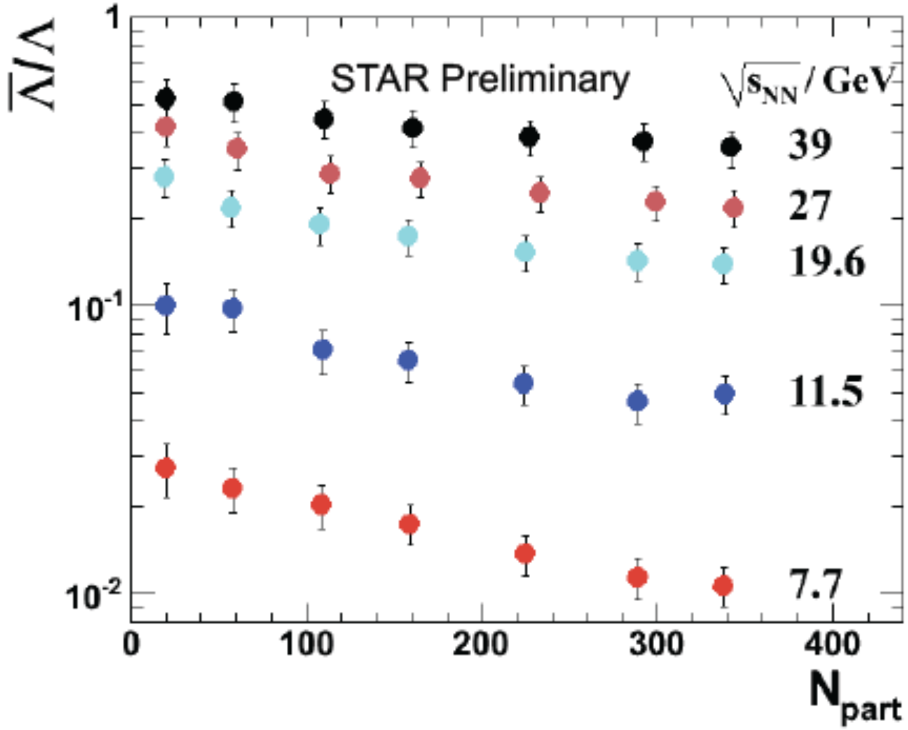

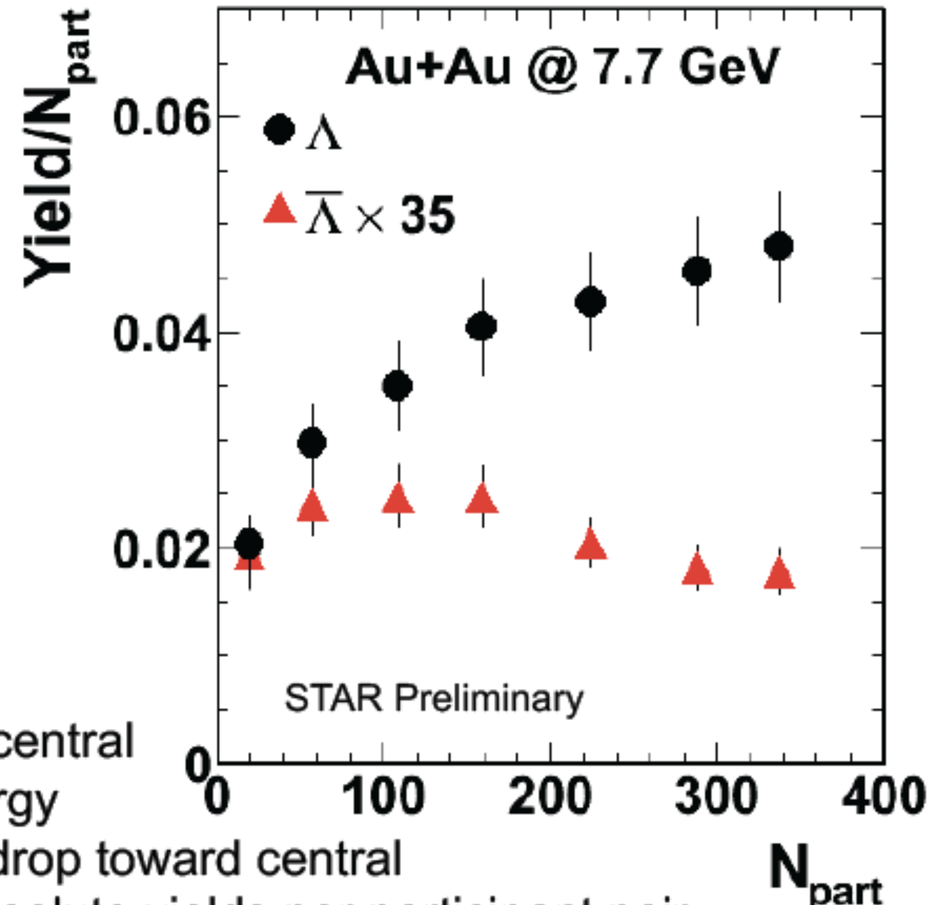

- Baryon stopping increases toward more central
- Stopping is more prominent at lower energy

It is believed that Absorption drives Bbar/B drop toward central
However, very little change of antibaryon absolute yields per participant pair

Important to understand initial stopping and pair production vs final state
7.7GeV COM energy => Fixed target Energy **31GeV proton** beam
p, phi, Lambda, Xi, Omega (antiparticle) production in p+A

Excitation function of antibaryon/baryons

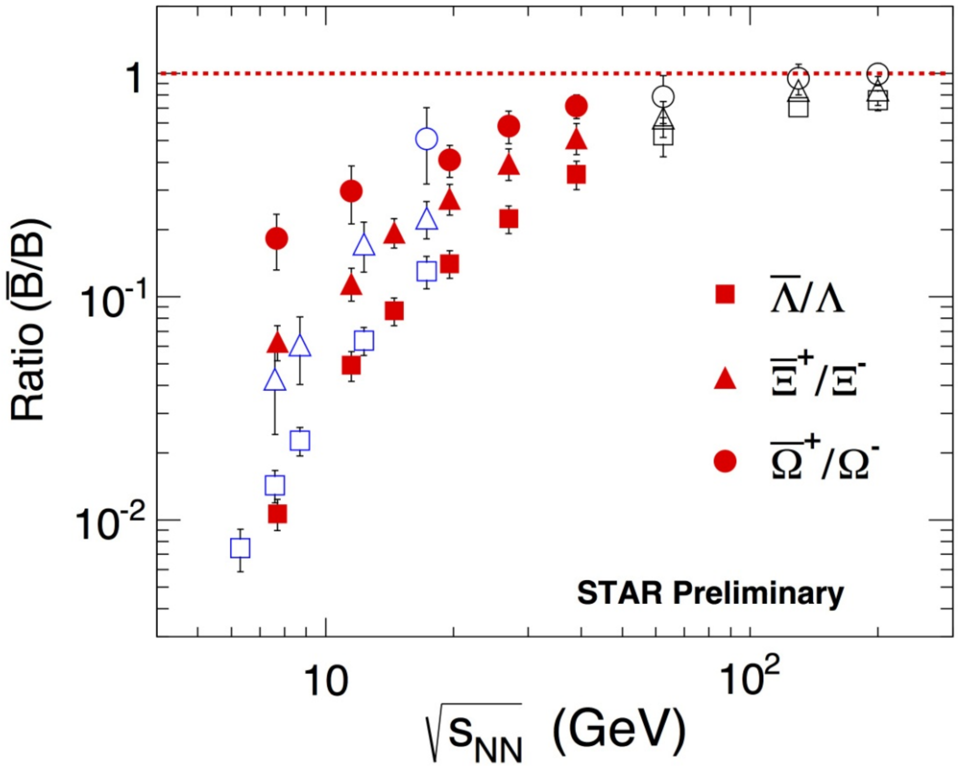

Statistical + systematical error

Left: Solid red: STAR BES; Solid blue: STAR published; Open blue: NA49

- STAR BES data lie in a trend with NA49 data
- $\overline{B}/B$ ratios increase with number of strange quarks at low energies $\overline{\Omega}^{+}/\Omega^{-} > \overline{\Xi}^{+}/\Xi^{-} > \overline{\Lambda}/\Lambda$

Anti-baryon to baryon ratio

$$n_i = \frac{g_i}{(2\pi^2)} \gamma_S^{|S_i|} m_i^2 T K_2(m_i/T) \exp(\mu_i/T)$$

$$\frac{\overline{\Lambda}}{\Lambda} = \exp(-\frac{2\mu_B}{T} + \frac{2\mu_S}{T}) \quad \Rightarrow \quad \ln(\frac{\overline{\Lambda}}{\Lambda}) = -\frac{2\mu_B}{T} + \frac{2\mu_S}{T}$$

$$\frac{\overline{\Xi}^+}{\Xi^-} = \exp(-\frac{2\mu_B}{T} + \frac{4\mu_S}{T}) \quad \Rightarrow \quad \ln(\frac{\overline{\Xi}^+}{\Xi^-}) = -\frac{2\mu_B}{T} + \frac{4\mu_S}{T}$$

$$\frac{\overline{\Omega}^+}{\Omega^-} = \exp(-\frac{2\mu_B}{T} + \frac{6\mu_S}{T}) \quad \Rightarrow \quad \ln(\frac{\overline{\Omega}^+}{\Omega^-}) = -\frac{2\mu_B}{T} + \frac{6\mu_S}{T}$$

- T is the temperature.
- μ_B is the baryon chemical potential.
- μ_S is the strangeness chemical potential.

(arXiv:nucl-th/9704046v1 by J.Cleymans & Phys. Rev. C 71(2005)054901)

μ_B and μ_s correlation

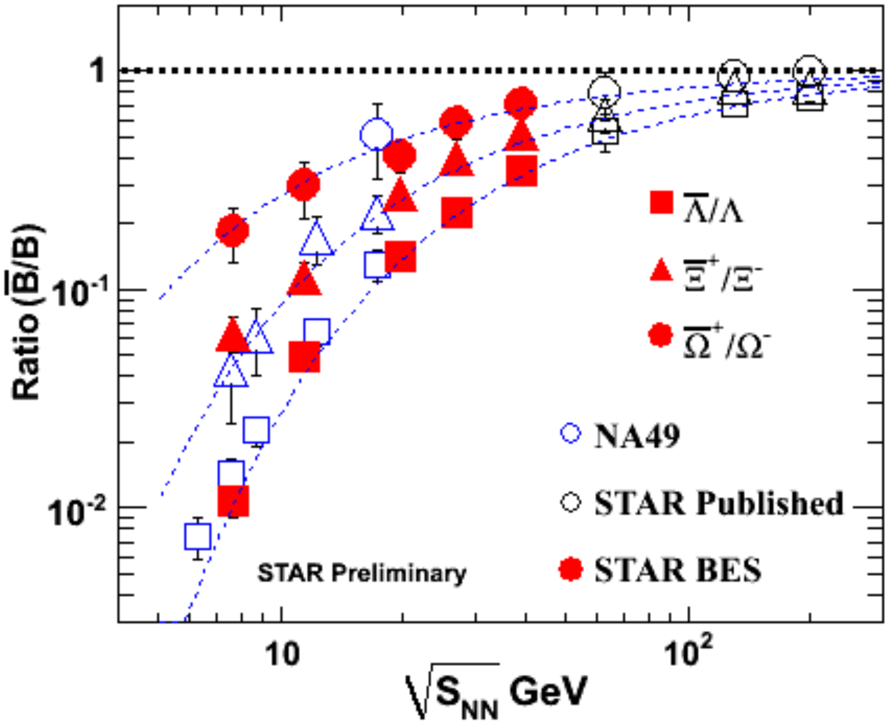

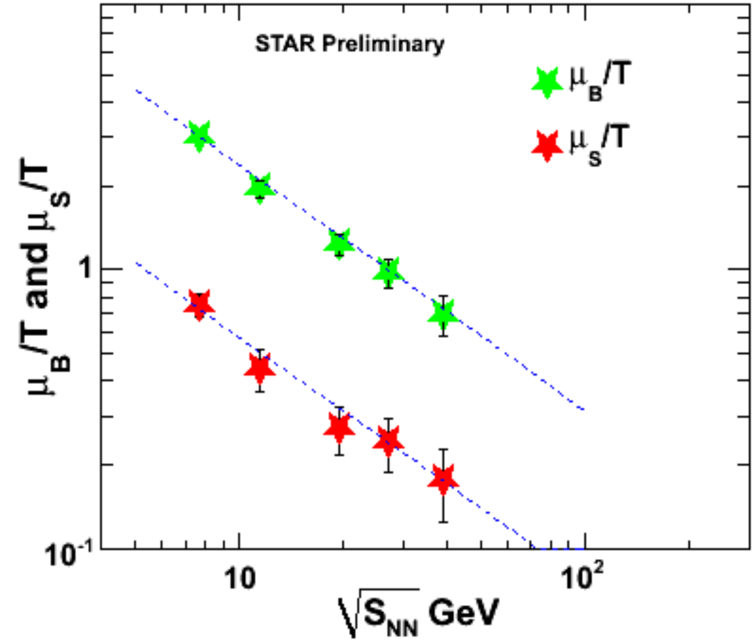

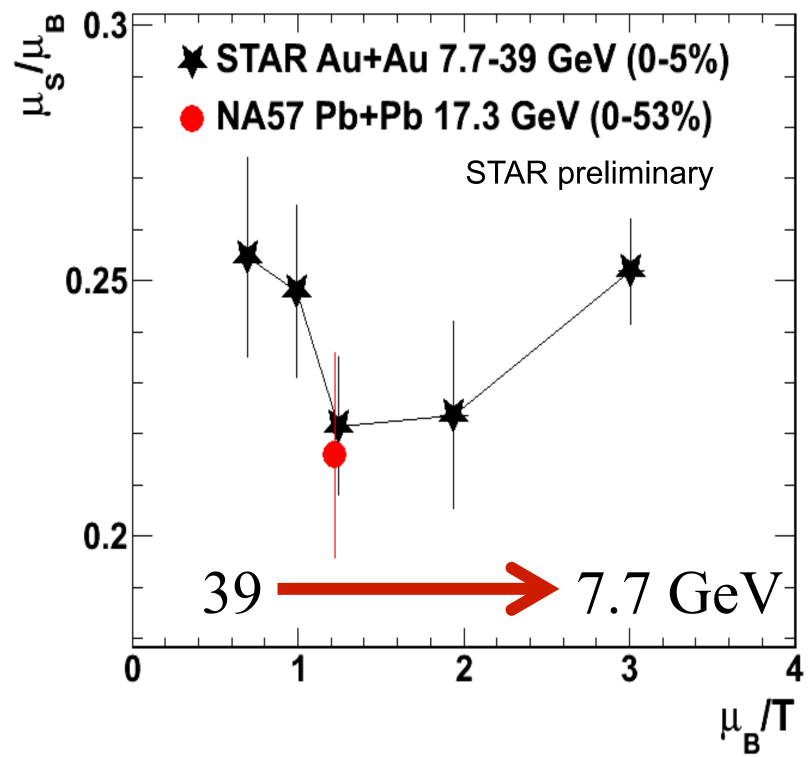

- Anti-baryon to baryon ratios are consistent with statistical thermal model
- $\mu_s/\mu B$ **seems to be smaller in 11.5 - 19.6 GeV than in 39 and 7.7 GeV**

Nuclear Modification Factors

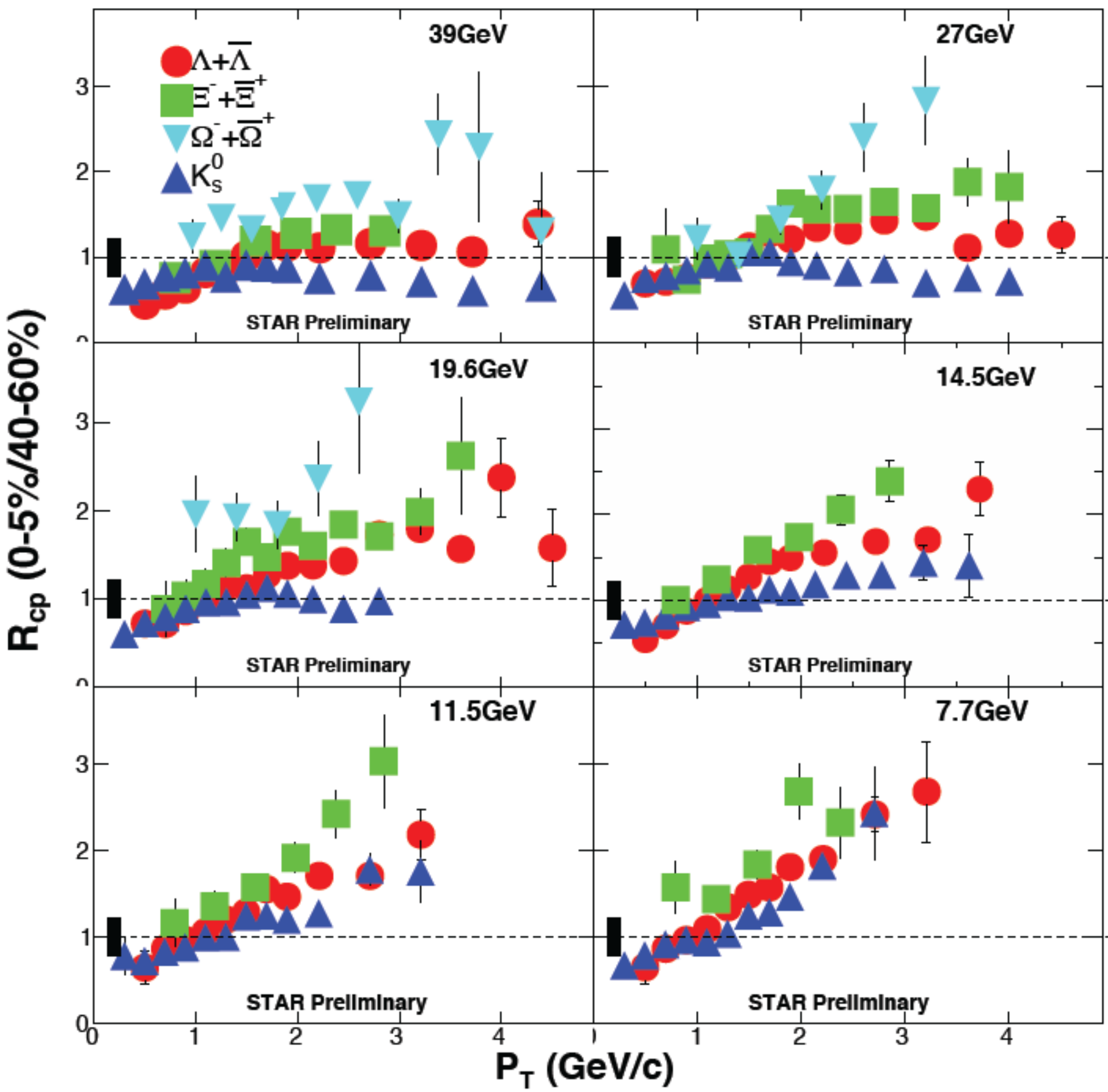

- $K_S{}^0$ R_{CP} increases with decreasing beam energies -> *the partonic energy loss effect less important in lower beam energy*
- The cold nuclear matter effect (Cronin effect) starts to take over at lower energies
- R_{CP} differences of particles becomes smaller at $\sqrt{s_{NN}} \leq$ 14.5 GeV -> indication of different properties of the system compared higher energies

$$R_{CP}(p_T) = \frac{[d^2\sigma/(N_{\rm bin} p_T dp_T dy)]_{\rm central}}{[d^2\sigma/(N_{\rm bin} p_T dp_T dy)]_{\rm peripheral}}$$

Nuclear modification factor: partonic energy loss and recombination

Strangeness Production

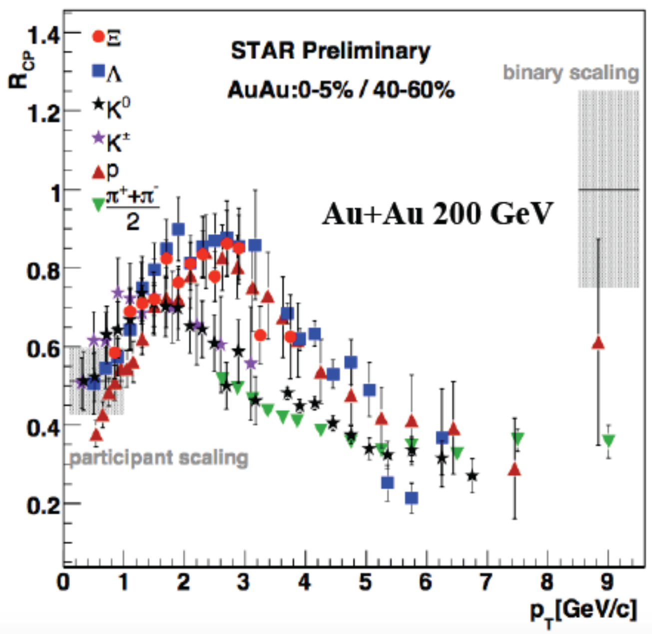

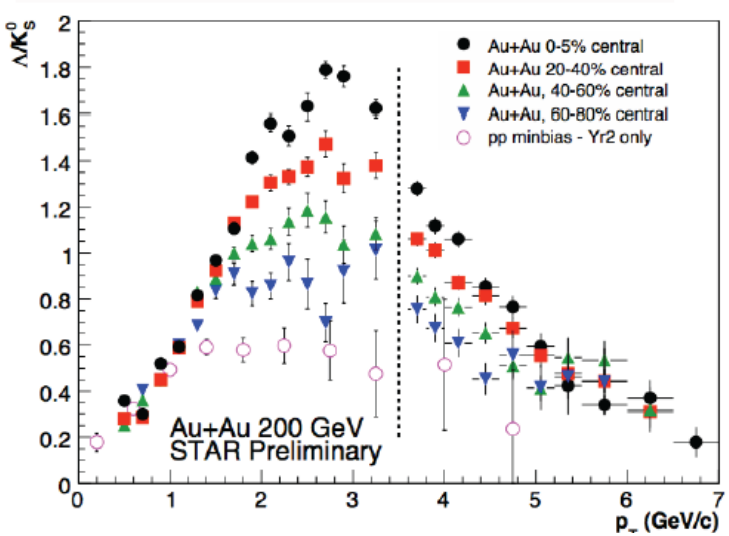

- Nuclear modification factors at Au+Au 200 GeV
  - Less than unity at high p_T
  - Baryon/meson follow different trends

  -> Partonic energy loss and recombination
- Baryon/meson ratio at Au+Au 200 GeV
  - Baryon enhancement at intermediate p_T in central collisions

  -> Parton recombination

Strangeness is sensitive probe

STAR: arXiv:1007.2613

$\bar{\Lambda}/K_S^0$ Ratio

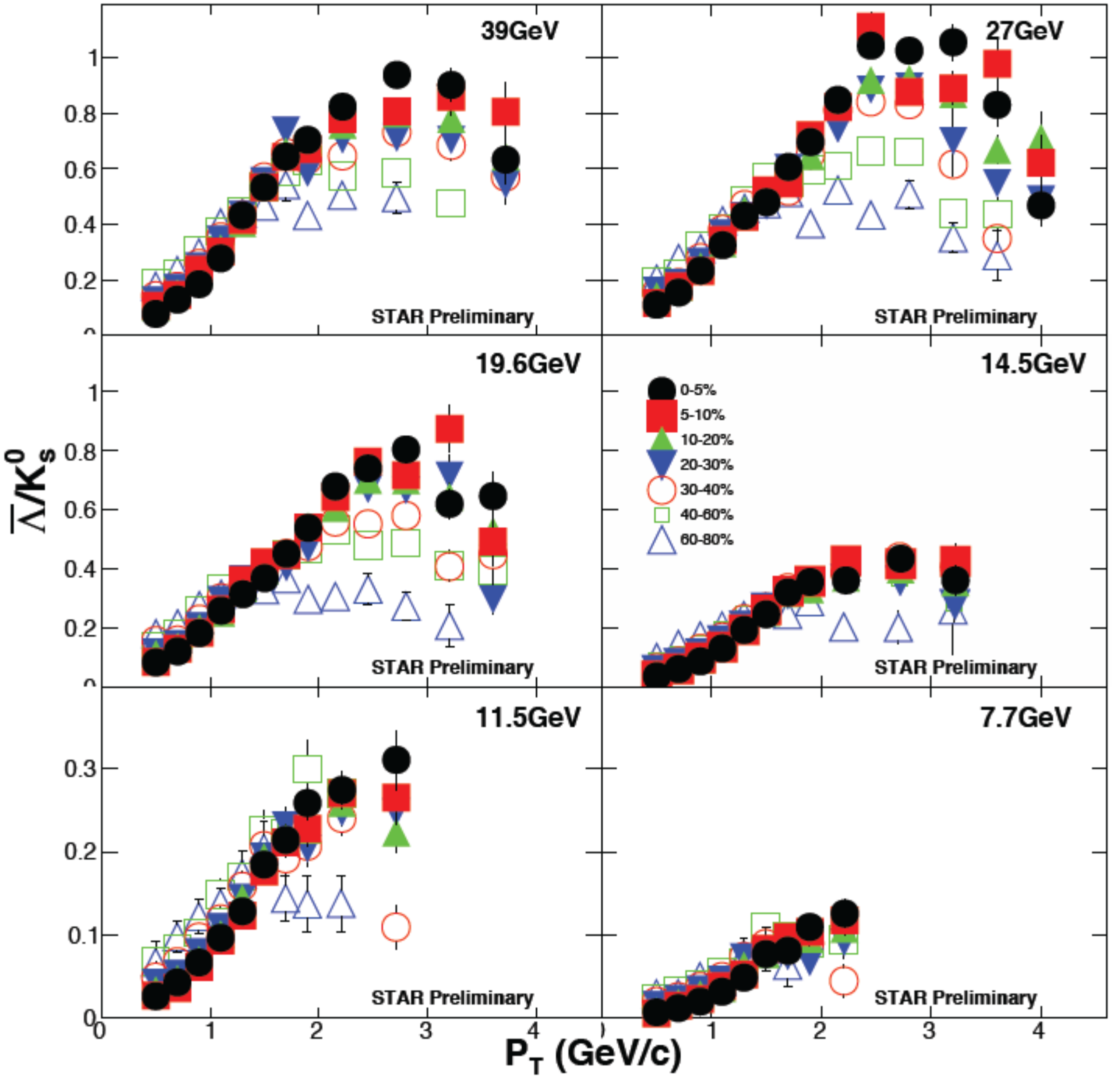

- The separation of central (0-5%) and peripheral (40-60%) collisions in the ratio less obvious when collision energy ≤ 14.5 GeV: less baryon enhancement

  ->

  possible change of medium property

- Need more statistics at lower beam energies

Enhancement of baryon at intermediate pT in central collisions: parton recombination

Ω / ϕ ratio

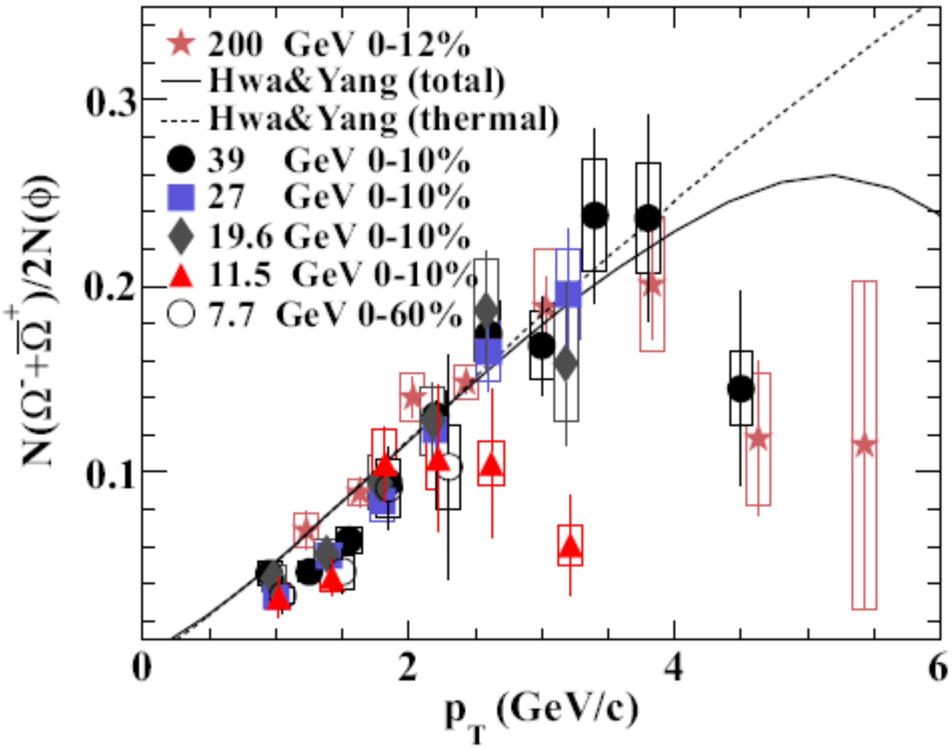

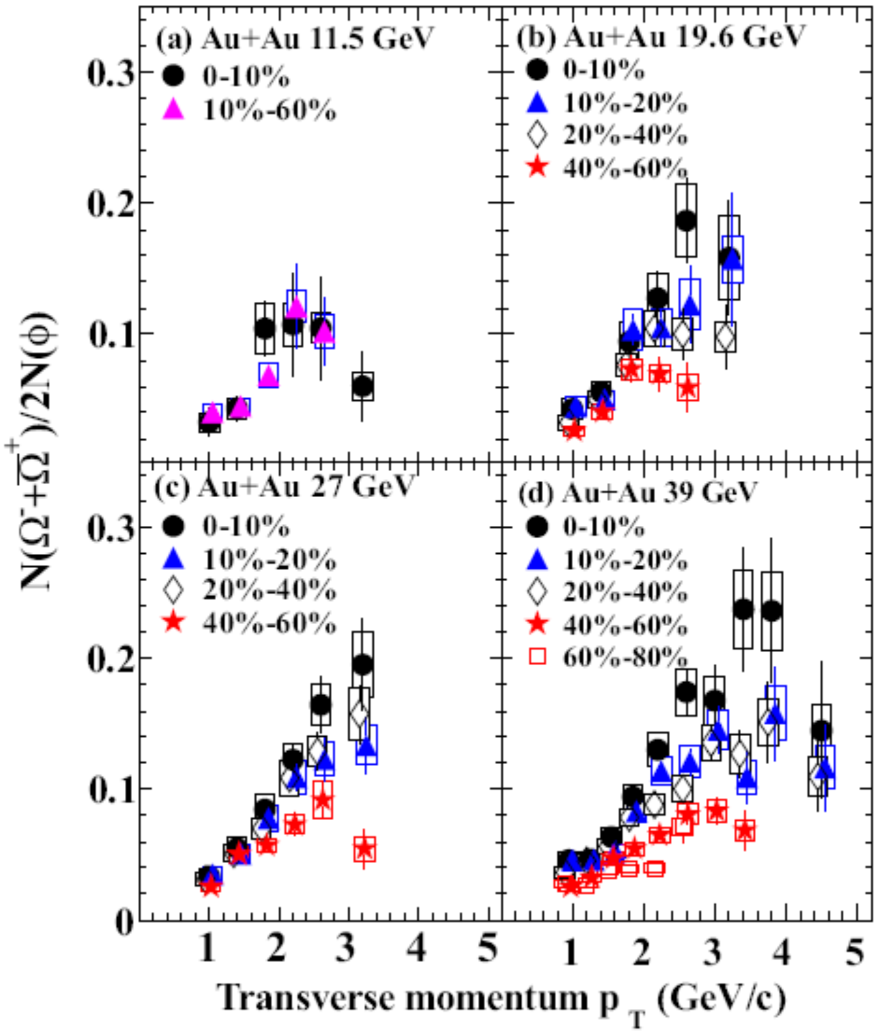

STAR, Phys. Rev. C 93, 2016, 021903 (R)

- Intermediate p_T Ω/ϕ ratios:
  Indication of separation between ≥ 19.6 and 11.5 GeV
- Ω/ϕ ratios: 40%-60% peripheral < 0-10% central for 19.6, 27 and 39 GeV

NCQ Scaled Ω/ϕ Ratio

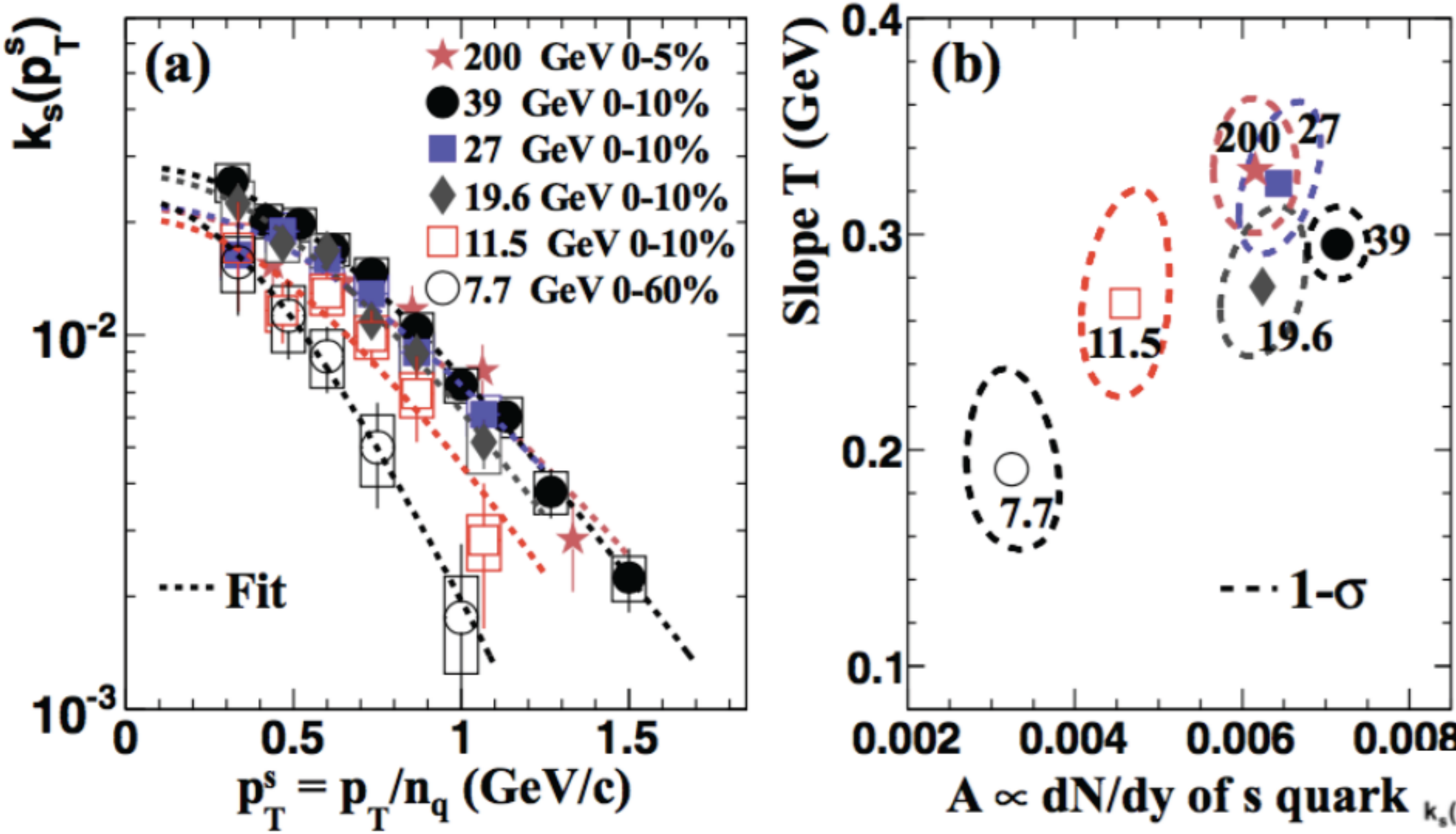

$$k_s(p_T^s) = \frac{N(\Omega^- + \overline{\Omega}^+)(p_T^{\Omega} = 3p_T^s)}{2N(\phi)(p_T^{\phi} = 2p_T^s)}$$

STAR: Phys. Rev. C 93, 021903 (2016)

- One single strange quark distribution describes both Ω and ϕ spectra-> quark coalescence production
- Slope (T) from Boltzmann fit changes at 7.7 GeV. *Centrality difference?*
- Decreasing *s* quark density below 19.6 GeV -> *Possible phase transition*

Ω Baryon and ϕ Meson v_2

Ω and ϕ: good probes of early partonic stage of collision

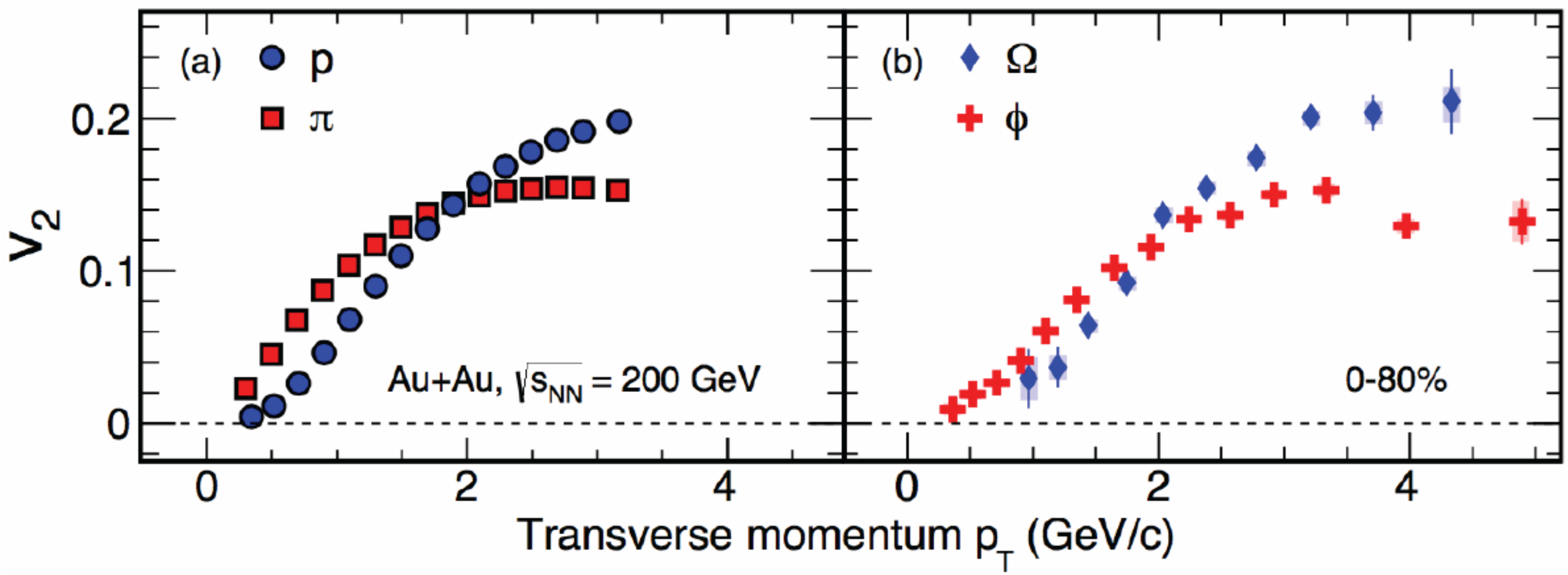

STAR: Phys. Rev. Lett.116, 062301 (2016)

- **Proton and pion v_2 compared with Ω baryon and ϕ meson v_2**
- **High precision data prove that Ω follows the baryon/meson splitting at intermediate p_T range, $2 < p_T < 5$ GeV/c .** ***First time!***

The major part of collectivity has been built-up at partonic stage!

The STAR Upgrades and BES Phase II

Major improvements for BES-II

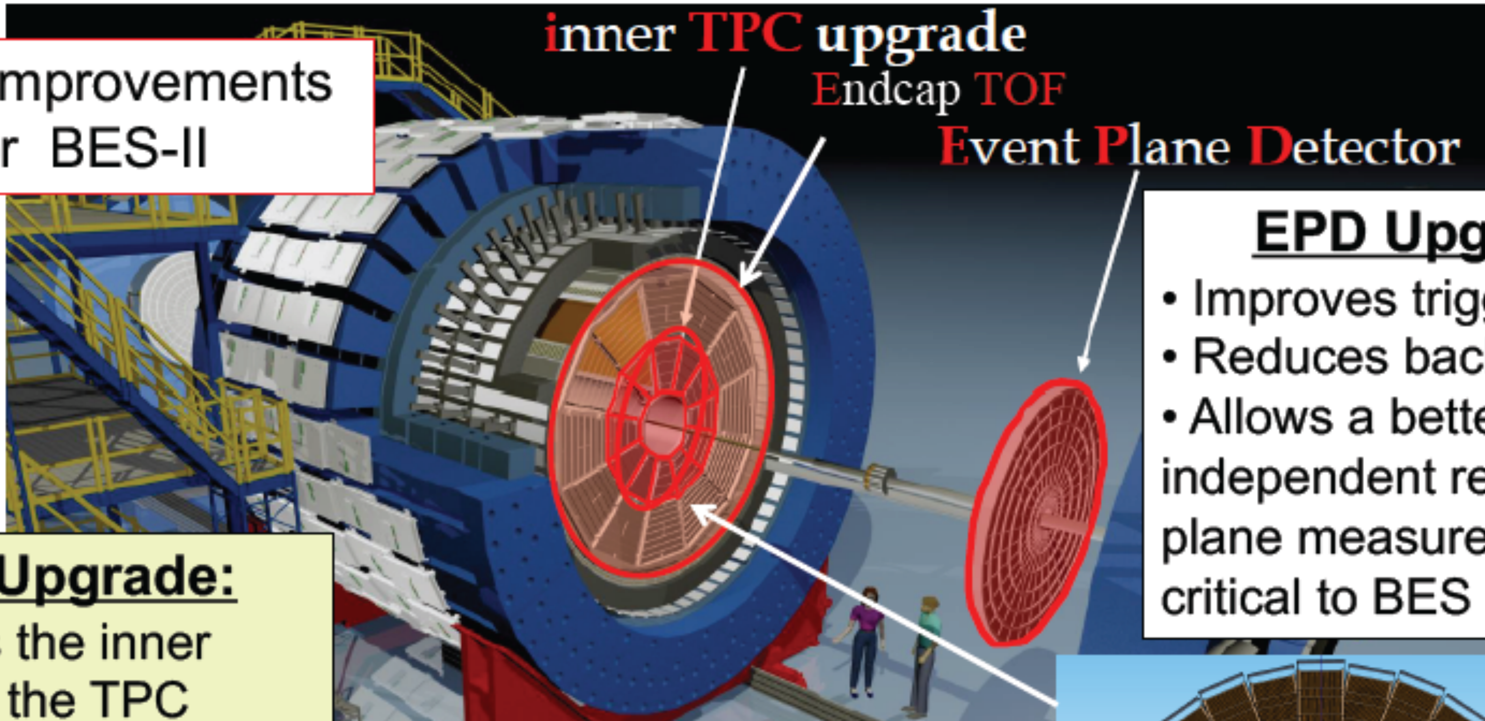

EPD Upgrade:

- Improves trigger
- Reduces background
- Allows a better and independent reaction plane measurement critical to BES physics

iTPC Upgrade:

- Rebuilds the inner sectors of the TPC
- Continuous Coverage
- Improves dE/dx
- Extends η coverage from 1.0 to 1.5
- Lowers p_T cut-in from 125 MeV/c to 60 MeV/c

EndCap TOF Upgrade:

- Rapidity coverage is critical
- PID at η = 0.9 to 1.5
- Improves the fixed target program
- Provided by CBM-FAIR

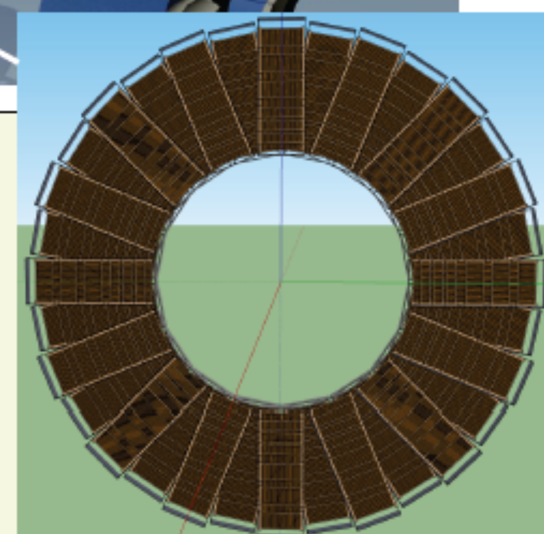

What is STAR iTPC upgrade?

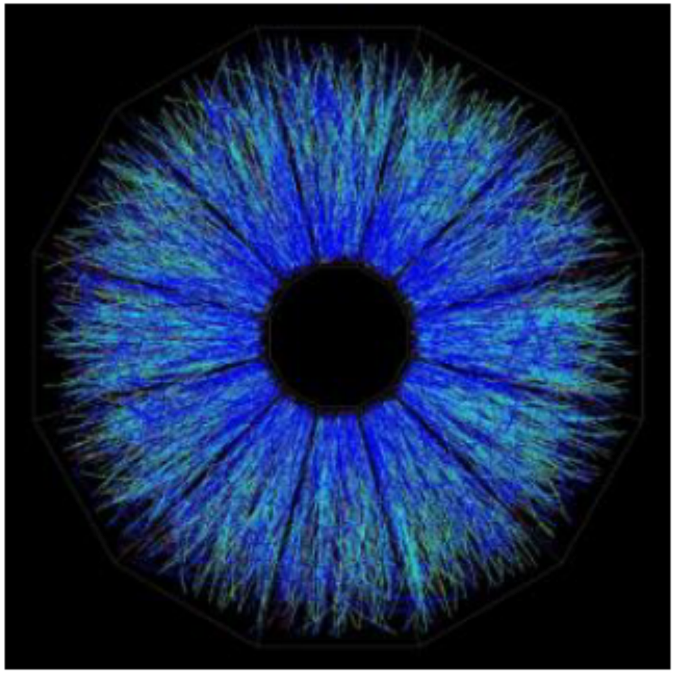

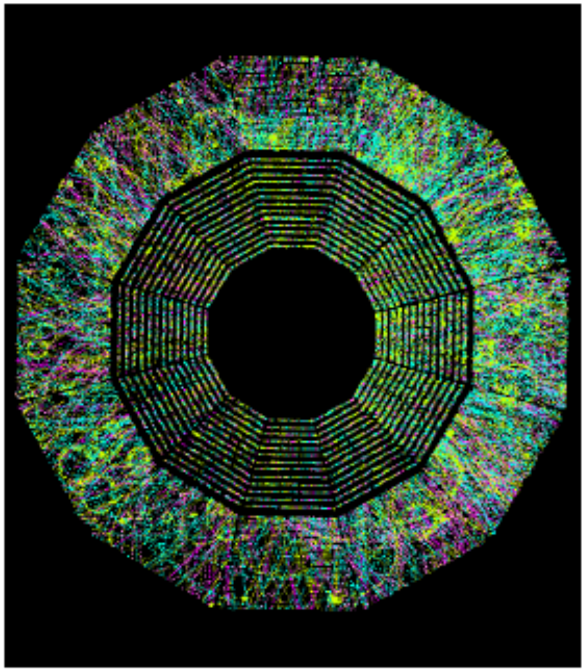

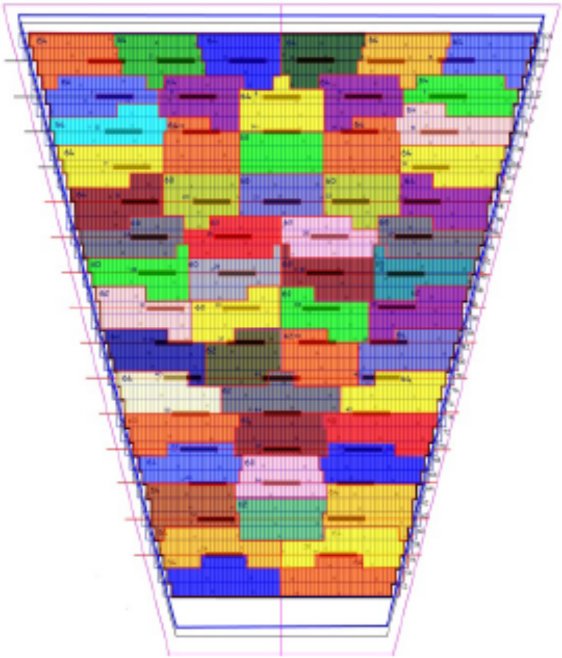

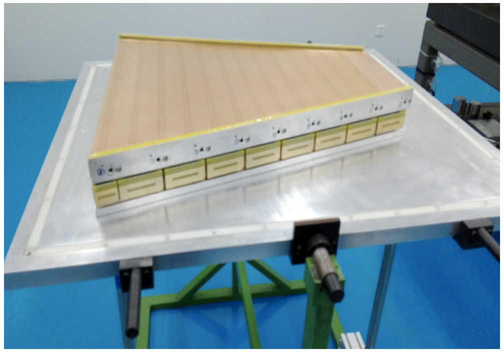

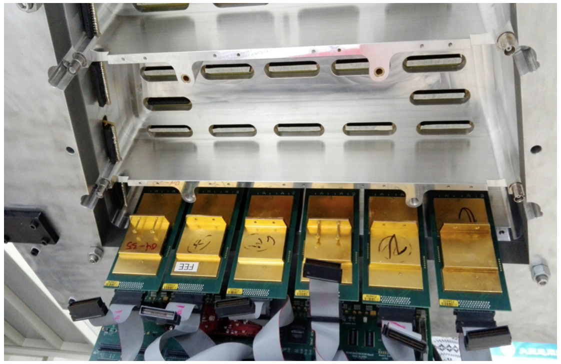

iTPC upgrade @Shandong Univ., China

Fixed Target Program with STAR

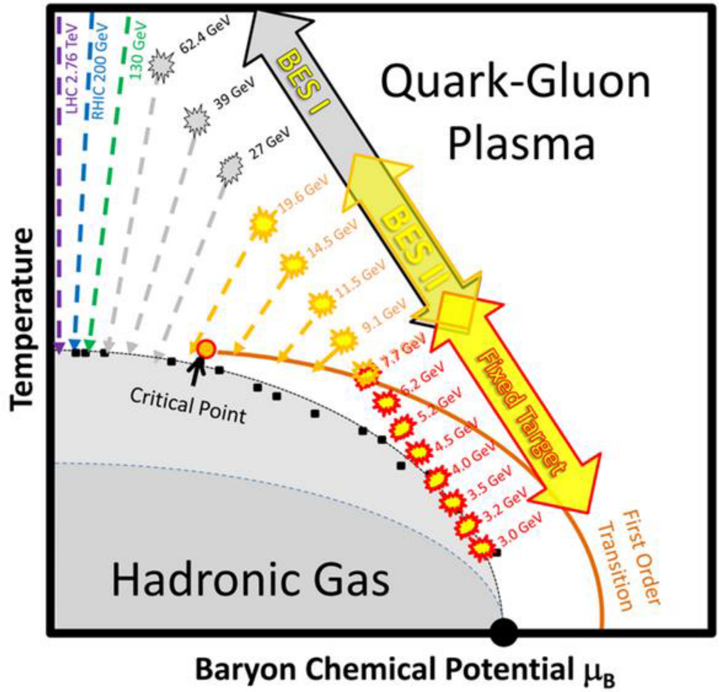

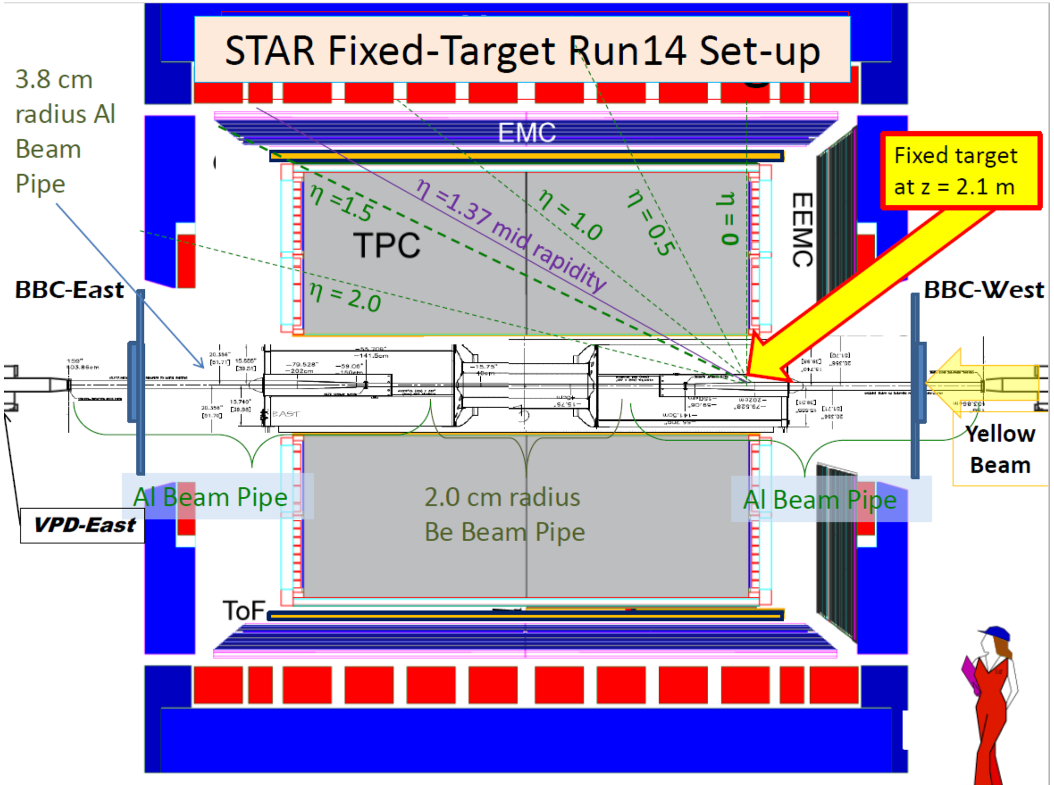

- Extend energy reach to overlap/complementary AGS/FAIR/JPARC
- Real collisions taken in run 14 and results (K. Meehan @ QM15 & WWND16)
- Upgrades (iTPC+eTOF+EPD) crucial
- Unprecedented coverage and PID for Critical Point search in BES-II
- Spectra, flow, fluctuations and correlations

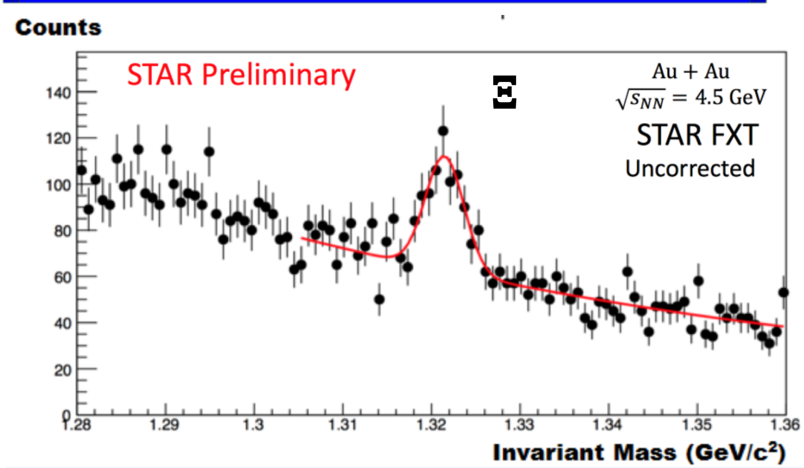

Summary

- Strangeness and hypernuclei are very exciting topics

- Strangeness is essential in determining
  the data point locations in QCD phase diagram
  Degree of thermalization from collisions to QGP
  Final-state absorption of antibaryons
  Global Polarization and Vorticity of the QGP fluid

- Looking forward to BES-II at RHIC, CBM, NICA and JPARC

Thank you for your attention